Biosensors and Bioelectronics 258 (2024) 116328

Contents lists available at ScienceDirect

Biosensors and Bioelectronics

journal homepage: www.elsevier.com/locate/bios

Softening implantable bioelectronics: Material designs, applications, and future directions

Subin Oh [a,1], Simok Lee [a,1], Sung Woo Kim [a], Choong Yeon Kim [a], Eun Young Jeong [a], Juhyun Lee [a], Do A Kwon [a,b], Jae-Woong Jeong [a,c,*]

[a] School of Electrical Engineering, Korea Advanced Institute of Science and Technology (KAIST), Daejeon, 34141, Republic of Korea
[b] Department of Materials Science and Engineering, Korea Advanced Institute of Science and Technology (KAIST), Daejeon, 34141, Republic of Korea
[c] KAIST Institute for Health Science and Technology, Daejeon, 34141, Republic of Korea

ARTICLE INFO

Keywords:
Softening
Implantable
Bioelectronics
Stimuli-responsive materials
Stiffness modulation

ABSTRACT

Implantable bioelectronics, integrated directly within the body, represent a potent biomedical solution for monitoring and treating a range of medical conditions, including chronic diseases, neural disorders, and cardiac conditions, through personalized medical interventions. Nevertheless, contemporary implantable bioelectronics rely heavily on rigid materials (e.g., inorganic materials and metals), leading to inflammatory responses and tissue damage due to a mechanical mismatch with biological tissues. Recently, soft electronics with mechanical properties comparable to those of biological tissues have been introduced to alleviate fatal immune responses and improve tissue conformity. Despite their myriad advantages, substantial challenges persist in surgical handling and precise positioning due to their high compliance. To surmount these obstacles, softening implantable bioelectronics has garnered significant attention as it embraces the benefits of both rigid and soft bioelectronics. These devices are rigid for easy standalone implantation, transitioning to a soft state *in vivo* in response to environmental stimuli, which effectively overcomes functional/biological problems inherent in the static mechanical properties of conventional implants. This article reviews recent research and development in softening materials and designs for implantable bioelectronics. Examples featuring tissue-penetrating and conformal softening devices highlight the promising potential of these approaches in biomedical applications. A concluding section delves into current challenges and outlines future directions for softening implantable device technologies, underscoring their pivotal role in propelling the evolution of next-generation bioelectronics.

1. Introduction

Implantable bioelectronics, seamlessly integrated within the body to interact directly with biological tissues and internal organs, hold immense promise across diverse applications. These encompass health monitoring (Yu et al., 2024), drug delivery (Joo et al., 2021), pacemaking (Ryu et al., 2021), neural interfacing (Jeong et al., 2015; Lee et al., 2020; Kim et al., 2021), hearing repair (Carlyon and Goehring, 2021), and cardiovascular stenting (Herbert et al., 2022b), which mitigate acute and chronic diseases, facilitate rehabilitation, and provide appropriate treatment that elevate the overall quality of patients' lives (Fig. 1a).

Conventional implantable devices are primarily constructed from rigid materials such as metals (e.g., Au, stainless steel, etc) and inorganic materials (e.g., Si, GaAs, etc). Owing to their rigid, bulky, and planar properties, these devices exhibit resistance to external forces, robustness, and static structures conducive to efficient surgical handling and implantation (Fig. 1b, top left). However, their inherent rigidity leads to severe inflammatory responses as well as tissue damage due to mechanical disparities with soft tissues (Someya et al., 2016) (Fig. 1b, middle left). The rigid form factor further hampers conformal integration with soft, curvilinear structures of internal organs, compromising stimulating and sensing performances (i.e., high impedance and low signal-to-noise ratio) (Pang et al., 2015) (Fig. 1b, bottom left). The paradigm shift towards soft implantable bioelectronics, emulating the mechanical properties of biological tissues with inherently soft and stretchable materials (Guo et al., 2022; Lee et al., 2022b), addresses these challenges. Such devices not only alleviate immunological side

* Corresponding author. School of Electrical Engineering, Korea Advanced Institute of Science and Technology (KAIST), Daejeon, 34141, Republic of Korea.
E-mail address: jjeong1@kaist.ac.kr (J.-W. Jeong).
[1] These authors contributed equally to this work.

https://doi.org/10.1016/j.bios.2024.116328
Received 18 February 2024; Received in revised form 30 March 2024; Accepted 22 April 2024
Available online 25 April 2024

effects by minimizing mechanical mismatches at the tissue-device interface (Fig. 1b, middle right) but also allow seamless attachment to various internal organs for precise physiological signal sensing and nerve stimulation (Li et al., 2021b; Sunwoo et al., 2021) (Fig. 1b, bottom right). Nevertheless, the inherent softness poses critical challenges in handling during surgical implantation (Fig. 1b, top right) and in achieving performance levels comparable to conventional rigid bioelectronics.

The key breakthrough lies in softening implantable bioelectronics, leveraging adaptive mechanical properties responsive to various stimuli (e.g., body temperature, bodily fluid, pH, enzymes, etc.). These softening devices seamlessly transition from an initial rigid state under off-body conditions to a softened state inside the body, combining the advantages of both rigid and soft devices. Their mechanical adaptability enables them to maintain their structures with high elastic modulus when outside the body, allowing for facile handling and precise positioning during implantation without the need for assistive tools. For example, tissue-penetrating softening implantable devices (e.g., neural probes) can be directly inserted into the target tissue without rigid stiffeners (Zhou et al., 2022; Park et al., 2021). Moreover,

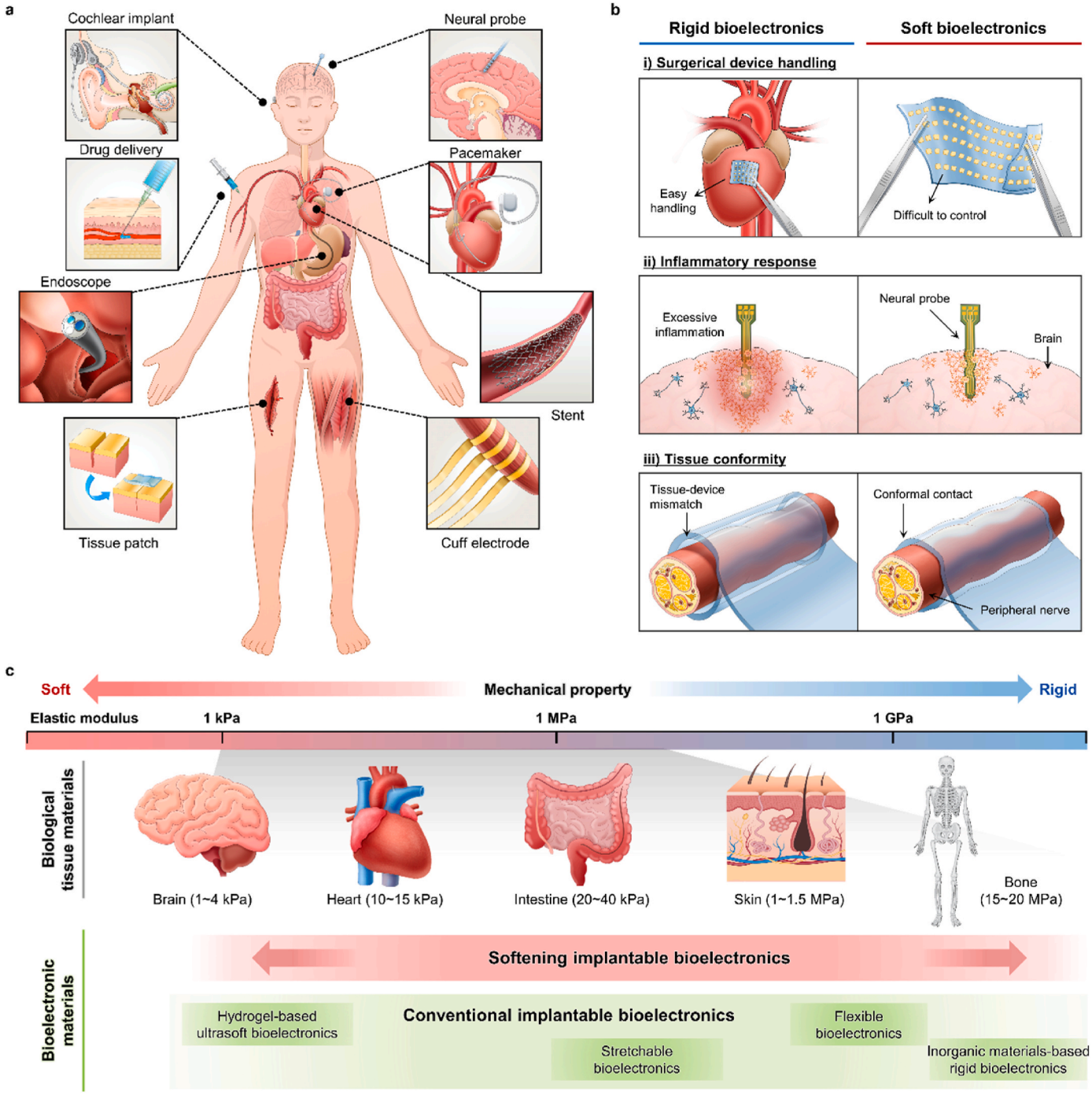

Fig. 1. Overall schematics of implantable bioelectronics illustrating challenges associated with electronics-tissue mechanical mismatch and the potential benefits of softening materials. a) Schematic illustration of conventional implantable bioelectronics, b) Advantages and disadvantages of recent implantable bioelectronics in the rigid (right) and soft (left) states, c) Mechanical variation range of softening materials in both rigid and soft states, highlighting their potential to address the limitations of traditional materials with invariant mechanical properties.

tissue-conformal softening implantable devices (e.g., nerve cuff), in their rigid state, exhibit easy handling and integration with the target organ surface with high mechanical stability (González-González et al., 2018). After implantation, the softened devices become pliable and malleable, establishing conformal contacts on tissues and minimizing discrepancies between biological tissues and the device (Jiao et al., 2023). The adaptive nature of softening devices enables versatile applications across diverse body parts, embracing a broad spectrum of mechanical properties of the human body with enhanced biocompatibility (Fig. 1c). Acknowledging the existence of various other effective methods for enhancing implantable device functionality and longevity, such as bioresorbable devices (Lee et al., 2021) and advanced encapsulation techniques (Kim et al., 2023), respectively, this review narrows its focus to the promising avenue of softening technologies, a field marked by active and ongoing research.

Despite recent reviews exploring various stiffness tunable materials for bio-integration, their applications in bio-integration and implantation remain largely unexplored. This review fills a crucial void by presenting a novel approach to softening implantable devices, focusing on stiffness-tunable materials with diverse softening mechanisms within *in vivo* conditions for implantable bioelectronics. We begin by discussing promising stiffness-tunable materials based on diverse softening mechanisms providing negligible impacts on the human body. Then, novel structural softening strategies and multifunctional features (e.g., self-healing, bio-adhesion) that emerge from softening approaches are briefly discussed. Next, real-world applications showcase the potential of tissue-penetrating and tissue-conformal softening implantable devices. The review not only addresses current challenges but also outlines future directions, making a significant contribution to the advancement of next-generation biomedical electronics.

2. Material designs for softening implantable bioelectronics

Understanding the chemical and mechanical properties of softening materials and their fundamental softening mechanisms is crucial for designing effective softening implantable bioelectronics. To create versatile softening bio-implantable systems that outperform current devices with static form factors (i.e., either rigid or soft in terms of mechanical properties), several key elements must be considered: wide stiffness variation, high processability and reliability, and the biocompatibility of softening stimuli. Achieving substantial stiffness modulation is paramount to fully leverage the advantages offered by both rigid and soft implantable devices. In off-body conditions, maintaining a high elastic modulus, akin to traditional rigid implantable devices (i.e., a few GPa or higher) ensures reliable device handling (Someya et al., 2016). Yet, upon implantation, rigidity must diminish to levels matching biological tissues (i.e., less than a few tens or hundreds of kPa), enhancing mechanical bio-intimacy at the biotic-abiotic interface. Softening materials play a pivotal role in fine-tuning device stiffness and should possess a high stiffness-tuning ratio exceeding 100-fold or more. Moreover, for seamless integration into existing implantable devices, these materials must exhibit high processability and chemo-mechanical stability, amplifying their versatility and widespread application. Furthermore, activation stimuli must align with *in vivo* conditions to mitigate any potential damage to biological tissues, requiring considerations such as adequate temperature (~37 °C), compatibility with biofluid, enzymes, pH, and magnetic field. By adhering to these criteria, precise and dynamic control over the stiffness of softening materials is achieved through mechanisms such as phase transition, conversion of molecular structures, adjustment of internal moisture content, and particle agglomeration. Additionally, as a structural mechanism, rigidity can be modulated by using a biodegradable material as a sacrificial layer. Table 1 outlines potential softening materials based on the aforementioned criteria, including activation stimuli, stiffness variation, and biocompatibility. This section provides a comprehensive exploration of diverse softening materials and designs, highlighting their strengths while addressing any associated limitations.

2.1. Softening materials based on phase transition mechanism

Phase transition, an entropically induced mechanism, intricately regulates the molecular motions of materials to effectively configure their mechanical properties (Gao et al., 2022; Zhao et al., 2015; Su et al., 2015). Within this realm, phase transition-based softening materials (PTSM) include shape memory polymers (SMPs), liquid crystal elastomers (LCEs), liquid metals, and gels. In the following sections, we will examine these softening materials and delve into their respective phase transformation approaches, showcasing the breadth and depth of their potential applications.

2.1.1. Shape memory polymer

SMPs, an emerging class of softening materials, undergo phase transition between liquid and solid states at the melting temperature (T_m) or between glassy and rubbery states at the glass transition temperature (T_g) (Wang et al., 2018). This transition is driven by the polymer chains within SMPs, which respond to thermal stimuli and exhibit variable mobility (Xue et al., 2022; Gao et al., 2022). Below the phase transition temperature, these polymer chains form a highly grafted network structure. However, beyond the transition temperature, the increased mobility of polymer chains facilitates macroscopic molecular motion and randomness within the polymer networks. The extensive degrees of stiffness modulation in SMPs are achieved by these large-scale transitions in chain configuration.

SMPs showcase two distinctive phase transition behaviors: glass transition (Byun et al., 2020) and first-order phase transition (melting process, in this case). The glass transition is a kinetic phenomenon (i.e., second-order thermodynamic transition) that offers relatively small stiffness modulation with a gradual phase transition (i.e., continuous entropy change) at T_g (Jiao et al., 2023; Qiu et al., 2020; Ren et al., 2016; Mattmann et al., 2022; Ware et al., 2012a; Zhang et al., 2015). During melting, however, polymers undergo a discontinuous phase transition by absorbing large amounts of latent heat, leading to a wide variation in elastic modulus at T_m (Zhao et al., 2017a, 2017b). For instance, Jiao et al. (2023) proposed multifunctional softening bioelectronics using polyurethane (PU)-based SMP substrates, which rely on glass transition for sensing physiological signals such as electrocorticography (ECoG) and electrocardiogram (ECG) (Fig. 2a). These PU-based SMPs exhibit a T_g of 38 °C close to body temperature (Fig. 2a, bottom left). In their rigid states at temperatures below T_g, their elastic modulus is approximately 100 MPa, allowing a facile 2D fabrication process for bioelectronics. After *in vivo* implantation, the SMP substrate rapidly achieves conformal contacts on a 3D curvilinear tissue surface, experiencing over a 100-fold reduction in elastic modulus (Fig. 2a, bottom right). Another exemplary case, proposed by Zhao et al. (2017a), features a thermodynamically softening biphasic synergistic gel (BSG) comprising stiffness-tunable micro-inclusions emulsified with a hydrogel matrix (Fig. 2b, top). The core component driving stiffness switch in BSGs is the micro-inclusions containing oleophilic stearyl methacrylate (SMA) monomers with long alkyl chains, facilitating thermodynamic melting-based transition (Fig. 2b, bottom left). Notably, a distinctive feature of BSGs is their high rigid-to-soft conversion ratio under biocompatible temperature conditions. The storage modulus of BSG decreases from 100 kPa to 20 kPa at its T_m of 38.6 °C (Fig. 2b, bottom middle and right).

SMPs stand out among other softening materials due to their substantial stiffness variation, ranging from hundreds of kPa and a few GPa, facilitated by phase transition mechanisms (Byun et al., 2020). Recent studies emphasize their remarkable chemical biocompatibility and processability, shedding light on their vast potential for applications in implantable devices (Ware et al., 2012a; González-González et al., 2018). In section 3, we delve into specific applications of SMPs in implantable bioelectronics, highlighting their potential as substrates for various devices like neural probes and nerve cuff electrodes to establish

Table 1
Comparison of various stimuli-responsive materials based on softening mechanisms.

	Material	Stimuli	Stiffness variation (max to min)	Modulus at body condition	Biocompatibility	Ref.
PTSM	Polycaprolactone diol (PCL), poly (hexamethylene diisocyanate) (PHMD), hexamethylene diisocyanate (HDI) - **SMP**	Heat (T_m = 38 °C)	100 MPa (R.T), 700 kPa (38 °C),	700 kPa (38 °C)	O	Jiao et al. (2023)
	Poly (vinyl acetate), cellulose nanocrystal **- SMP**	Fluid	3411 MPa (dry), 33 MPa (wet)	33 MPa (wet, 37 °C)	O	Harris et al. (2011)
	Stearyl acrylate (SA), Tetradecyl acrylate (TA), Urethane diacrylate (UDA) - **SMP**	Heat (T_m = 26–32 °C)	30.8 MPa (R.T), 0.03 MPa (body temp.)	30 kPa	O	Gao et al. (2021)
	Bacterial cellulose, Carboxyethyl acrylate (CEA) **- SMP**	Fluid (polar solvent), Heat (T_m = 30–43 °C)	~1.5 GPa (dry, R.T), 69 kPa (water, 50 °C)	~40 kPa (wet, 37 °C)	O	Qiu et al. (2020)
	Stearyl acrylate (SA), Tetradecyl acrylate (TA), Urethane diacrylate (UDA) - **SMP**	Heat (T_m = 34–46 °C)	28 MPa (R.T), 0.38 MPa (above T_m)	0.38 MPa (37 °C)	–	Ren et al. (2016)
	Nanoclay, N,N-dimethylacrylamide (DMAA), Stearyl methacrylate (SMA), Ethylene glycol dimethacrylate (EGDMA) **- SMP**	Heat (T_m ~ 38.6 °C)	~100 kPa (below T_m), ~20 kPa (above T_m)	~50 kPa (37 °C)	–	Zhao et al. (2017a)
	Nanoclay, DMA, Lauryl methacrylate (LMA), EGDMA, paraffin **- SMP**	Heat (T_m = 54–57 °C)	0.57 MPa (20 °C), 0.053 MPa (70 °C)	- (>0.12 MPa)	–	Zhao et al. (2017b)
	Methyl acetate (MA), Isobornyl acrylate (IBoA), poly (ethylene glycol) diacrylate, Acrylic acid (AA) - **SMP**	Fluid, Heat (T_g ~ 60 °C)	~700 MPa (dry, 37 °C), ~100 kPa (dry, 100 °C)	~0.3 MPa (wet, 37 °C),	–	Ware et al. (2012a)
	Acrylonitrile (AN), Acrylamide (Aam), 2-acrylamido-2-methyl-1-propanesulfonic acid (AMPS) - **SMP**	Heat (>15 °C)	~18 MPa (10 °C), ~210 kPa (60 °C)	~1 MPa (35 °C)	–	Zhang et al. (2015)
	RM82, 2,2'-(ethylenedioxy) diethanethiol (EDDT), TATATO - **Liquid crystal**	Heat (T_{Ni} = 35 °C)	>1 GPa (−20 °C) ~ 0.7 MPa (30 °C)	~0.7 MPa	–	Saed et al. (2019)
	RM82, n-butylamine, polyrotaxane **- Liquid crystal**	Heat (T_{pm} ~58 °C)	~200 MPa (−25 °C), ~0.3 MPa (100 °C)	~5 MPa	–	Choi et al. (2022)
	RM82, n-butylamine **- Liquid crystal**	Heat (T_{Ni}: 95 °C)	~50 kPa s (R.T), ~200 Pa s (120 °C)	10–50 kPa s	–	Kotikian et al. (2018)
	RM257, EDDT **- Liquid crystal**	Heat	~1 GPa (<0 °C), ~0.3 MPa (~50 °C)	~1 MPa	–	Mistry et al. (2021)
	RM257, EDDT, (mercaptopropyl)methylsiloxane (PMMS) **- Liquid crystal**	Heat (T_g = 30 °C)	~1 GPa (−25 °C), <1 MPa (~80 °C)	~10 MPa	–	Zhang et al. (2020)
	Gallium **– Liquid metal**	Heat (T_m = 29.8 °C)	9.8 GPa (below T_m), ~0 Pa (above T_m)	~0 Pa (37 °C)	O	Wen et al. (2019); Agno et al. (2023)
	Tendon gelatin (TG), 2-ureido-4 [1H]-pyrimidinone unit (UPy unit) - **Gel-sol transition**	Heat (T_{trans} = 40 °C)	~20 kPa (20 °C), 100 Pa (40 °C)	~1 kPa (37 °C)	O	Nishiguchi et al. (2022)
	APmoc-F(CF3)F, Enzyme activation system (EAT) **- Gel-sol transition**	Non-enzymatic protein (avidin)	2300 Pa (w/o bCAII), 770 Pa (w/bCAII)	770 Pa (w/bCAII)	–	Shigemitsu et al. (2020)
MCSM	PDMS–COO–Zn	Heat (T_g = 55.7 °C)	800 MPa (25 °C), 0.9 MPa (80 °C)	~500 MPa	–	Lai et al. (2018)
	Cellulose-graft-poly (n-butyl acrylate-*co*-1-vinylimidazole) (Cell-P(BA-*co*-VI)), Cu2+	Heat (T_g = 27.6 °C)	~400 MPa (~- 60 °C), ~1 MPa (~80 °C)	~2 MPa	–	Wang et al. (2020a)
	Thioctic acid (TA), 1,3-diisopropenylbenzene (DIB), Fe^{3+}	Heat	~0.2 MPa (30 °C), ~10 kPa (100 °C)	~0.2 MPa	O	Zhang et al., 2018b
	Lyophilized silk proteins	Fluid	38.7 MPa (dry), 3.53 MPa (wet)	3.53 MPa (wet)	O	Zhou et al. (2022)
	Poly (styrene-*co*-butadiene) (SBR), sulfonated whiskers	Fluid	236 MPa (dry), 39 MPa (wet)	39 MPa (wet)	–	Dagnon et al. (2012)
	Polyurethane	Heat (T_g < 0 °C)	>1 GPa (~−40 °C), ~1 MPa (~40 °C)	~1 MPa	–	Chen et al. (2020)
	Tricyclodecane dimethanol diacrylate (TCMDA), 1,3,5-triallyl-1,3,5-triazine-2,4,6(1H,3H,5H)-trione (TATATO), 2,2,-dimethoxy-2-phenyl acetophenone (DMPA), Tris [2-(3-mercaptopropionyloxy)ethyl] isocyanurate (TMICN)	Fluid, Heat (T_g = 60 °C)	600 MPa (dry, 25 °C), 4 MPa (wet, 70 °C)	80 MPa (wet, 37 °C)	O	Reeder et al. (2014)
	2,2,2-trifluoroethyl methacrylate (TFEMA), 2,2,3,4,4,4-hexafluorobutyl acrylate (HFBA)	Heat (T_g = 12.1 °C)	~1 GPa (~10 °C), ~1 MPa (~60 °C)	~100 Mpa	–	Liu et al. (2022b)
	Poly (acrylic acid) (PAA), branched poly (ethylenimine) (bPEI) - pH	pH 6	~300 MPa (pH 2), ~30 MPa (pH 6)	~30 MPa (pH 6), depends on pH environment	–	Kim et al. (2016)

(*continued on next page*)

Table 1 (*continued*)

	Material	Stimuli	Stiffness variation (max to min)	Modulus at body condition	Biocompatibility	Ref.
	poly (2-(diisopropylamino)ethyl methacrylate) (PDPA), poly (2-(methacryloyloxy)ethyl phosphorylcholine) (PMPC) - > ABA triblock copolymer - pH	pH 7	40 kPa (pH 8), 1.4 kPa (pH 7)	1.4 kPa (pH 7)	O	Yoshikawa et al. (2011)
Swelling	Poly (acrylamide)-alginate (PAAM-Alg) - **Swelling**	Fluid	50 MPa (dry), 16.5 kPa (wet)	16.5 kPa	O	Park et al. (2021)
	polyacrylamide (PAAM) - **Swelling**	Fluid	~700 kPa (dry), <100 kPa (wet)	<100 kPa (wet)	–	Xu et al., 2023b
	poly (hydroxyethyl)methacrylate (PHEMA) - **Swelling**	Fluid	1 GPa (dry), 0.3 MPa (wet)	0.3 MPa (wet)	O	Opdahl et al. (2003)
	β -cyclodextrin modified alginate (β -CD-Alg), diethylenetriamine modified alginate (DETA-Alg) - **Swelling** & pH	Fluid, (pH 7)	627.24 MPa (dry), 2.89 MPa (wet)/5.07 MPa (pH 11.5), 2.89 MPa (pH 7)	2.89 MPa (wet, pH 7)	O	Han et al. (2012)
	SUP705, RGD8530, TangoBlackPlus - **Swelling & metamaterial**	Fluid	~300 kPa (dry), nearly 3 orders of magnitude decreased (wet)	~300 Pa (wet)	–	Zhang et al. (2018a)
	Alg-GMA (glycidyl methacrylate), N-vinylpyrrolidone (VP), Sodium acrylate (SA) - pH	pH 7.4	Swelling degree (mass) ~900% (Alg1V2A1 at pH 7.4)	Modulus information not available [Swelling ratio (mass) ~900% (Intestinal fluid: pH 7.4, 37 °C)]	O	Lima et al. (2018)
	carboxymethyl chitosan (CMCS), water soluble dynamer (obtained by benzene-1, 3, 5-tricarbaldehyde (BTA), di-amino Jeffamine) - pH	pH > 5	Swelling ~7500% (at pH 8), <500% (at pH 3)	Modulus information not available [Swelling ratio ~2000% (at pH 7.4)]	O	Yu et al. (2021)
	Glutamic acid grafted chitosan (CH-g-GA) hydrogel beads - pH	pH 2.1, 5.8, 7.4	Swelling ~ 104.5% (at pH 2.1), ~426% (at pH 5.8)	Modulus information not available [Swelling ratio ~309.8% (at pH 7.4)]	O	Nisar et al. (2021)
Jamming	gelatin glycidyl methacrylate (GelGMA), hyaluronic acid glycidyl methacrylate (HAGMA), thiol-coated magnetic microparticle (MMP) - **magnetic field**	Magnetic field (~1 T)	2640 Pa (w/magnetic field), 560 Pa (w/o magnetic field)	560 Pa (w/o magnetic field)	O	Shou et al. (2023)
Biodegradable material	Silk fibroin	Fluid, enzyme	3~17 GPa (depends on silk sericin content) (dry), ~0 Pa (wet, proteolytic enzyme)	~0 Pa (wet, proteolytic enzyme)	O	Cointe et al. (2022); Kim et al. (2010); Cao and Wang, 2009
	Magnesium	Fluid	42 GPa (dry), ~0 Pa (wet)	~0 Pa (wet)	O	Zhang et al. (2023b)
	Spin-on-Glass (SOG)	Fluid	14 GPa (dry), ~0 Pa (wet)	~0 Pa (wet)	O	Hosseini et al. (2021); Kang et al. (2015)
	poly-4-hydroxybutyrate (P4HB)	Fluid, enzyme (lipase)	70 MPa (dry), ~0 Pa (wet, enzyme)	~0 Pa (wet, enzyme)	O	Keridou et al. (2020)
	Poly (vinyl alcohol) (PVA) film	Fluid	3.4 GPa (dry), ~0 Pa (wet)	~0 Pa (wet)	O	Kim et al. (2020)
	Magnesium oxide (MgO)	Fluid	300 GPa (dry), ~0 Pa (wet)	~0 Pa (wet)	O	Hwang et al. (2015)

a *Modulus at body condition*: the maximum modulus of softening materials that can be achieved by *in vivo* implantation (under body conditions).

strong bio-mechanical affinity with tissues.

2.1.2. Liquid crystal elastomer

LCE is a crosslinked polymer network combining the elasticity of elastomers and the self-assembly of liquid crystals. It involves rod-like molecular segments known as mesogens, which are linked to either main or side chains of polymer networks. LCEs undergo phase transitions between ordered states (nematic or smectic) and disordered states (isotropic) depending on the orientational and positional configurations of mesogens (Herbert et al., 2022a; Jayasri et al., 2009). The macroscopic alignment of mesogens governs the phase of the LCEs, while the dynamic fluctuation of liquid crystallinity and polymer chains modulates the stiffness and actuation of LCEs (Wang et al., 2020b; Choi et al., 2022; Kotikian et al., 2018; Mistry et al., 2021). For example, Li et al. (2021a) introduced a 3D-printed LCE soft actuator capable of stiffness tuning and programmable locomotion. To create this soft actuator, a photopolymerizable LCE liquid resin is employed, composed of diacrylate LC monomers (RM257), dithiol linker (EDDT), and trivinyl cross-linker (TATATO). These components are printed in layers by applying a shear force to ensure highly aligned LCEs. Heating the LCE above its critical transition temperature (T_{NI} ~ 39 °C) induces a shift from the well-organized mesogens and polymeric chains (i.e., nematic

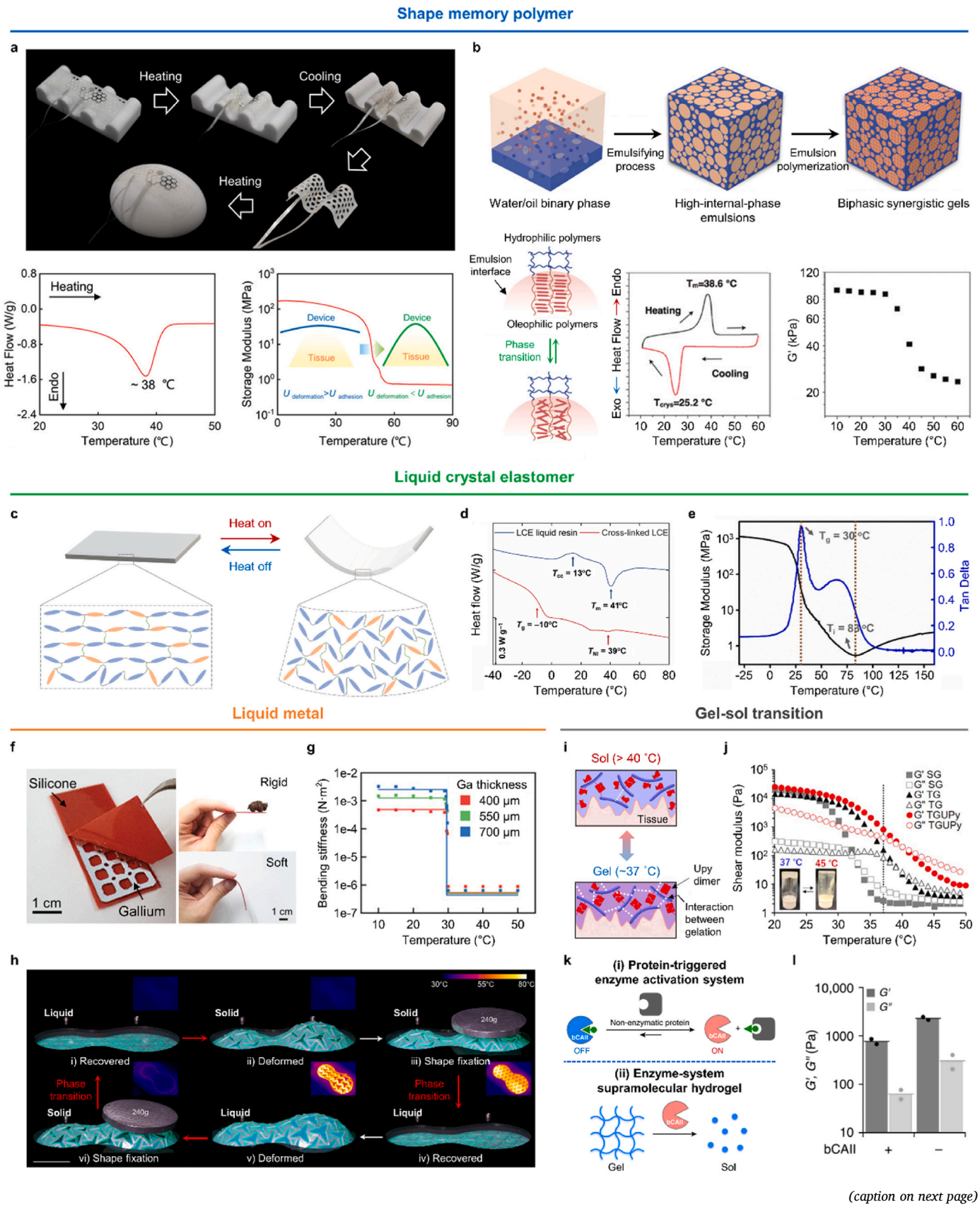

(caption on next page)

Fig. 2. Softening materials through phase-transition mechanisms. a) Shape memory polymer (SMP) based on polyurethane that can reversibly tune its rigidity in response to temperature using phase-transition properties. Sequential photographs (top) highlighting the abilities of stiffness modulation as well as shape transformation of SMP, which is induced by thermal stimuli. Differential scanning calorimetry (DSC) curve of SMP exhibiting the melting temperature (T_g: ~38 °C) (bottom left). Temperature-dependent storage moduli of SMP (bottom right) (Jiao et al., 2023) (Copyright, 2023; Wiley). b) Biphasic synergistic gel (BSG), which consists of closely packed semicrystalline micro-inclusions within a soft hydrogel matrix, showing a softening mechanism underlying on phase-transition. Schematic illustrations (top) of the synthesis process of BSGs based on in situ polymerization of high-internal-phase emulsions. Illustration of the heterogeneous interface between micro-inclusions and hydrogel matrix during phase-transition (i.e., melting-to-crystallization or vice versa) of micro-inclusions (bottom left). DSC curve (bottom middle) and dynamic mechanical analysis (DMA) curve (bottom right) for BSGs depicting thermally responsive characteristic temperature (e.g., T_m, T_{crys}) and storage moduli (Zhao et al., 2017a) (Copyright, 2017; Wiley). c) Schematic showing the stiffness modulation principle of liquid crystal elastomer (LCE) based on isotropic-anisotropic (e.g., nematic, cholesteric, smectic, isotropic) phase transition mechanism and their concomitant bending actuation through thermal stimuli. Phase transformation is related to the reconfiguration of LCE polymeric network alignment and direction. d) DSC curve of LCE indicating glass transition temperature (T_g: ~ −10 °C) and nematic-to-isotropic transition temperature (T_{NI}: ~39 °C) (Li et al., 2021a) (Copyright, 2021; AAAS). e) Storage modulus and tan δ of thiol-acrylate Michael addition reaction-based LCE as a function of temperature (Zhang et al., 2020) (Copyright, 2020; AAAS). f) Representative liquid metal-based material that can modulate the rigidity arising from reversible liquid-solid phase transition. Optical images of a mechanically transformative platform consisting of a gallium-based frame with a silicone encapsulation (left) and demonstrating mechanical characteristics in rigid and soft states to emphasize the wide mechanical variation (right). g) Bending stiffness of the gallium-based platform as a function of temperature with varying the thickness of the gallium frame (Byun et al., 2021) (Copyright, 2021; Wiley). h) Sequential image illustrating the shape programming process of heavy metal-free low melting point alloy (LMPA)-embedded kirigami composite with varying mechanical properties through thermal stimuli. Heavy metal-free LMPA (e.g., Bi–Sn–In alloy) based softening material benefits to enhance biocompatibility (Hwang et al., 2022) (Copyright, 2022; AAAS). i) Schematic diagram illustrating the working mechanism of thermally responsive gel-sol transition of supramolecular materials based on TG functionalized with UPy. The gel-sol transition temperature can be controlled by the strength of hydrogen bonding, which is dominant in retaining the gel state network. j) Photographs indicating the rheological behavior of TG and TGUPy under body temperature (~37 °C). TGUPy exhibits a viscoelastic gel state at 37 °C, while TG is in a sol state. k) Shear modulus at varied temperatures of SG, TG, and TGUPy solution dissolved in PBS at 20 wt% (Nishiguchi et al., 2022) (Copyright, 2022; Elsevier).

phase) to disordered states (i.e., isotropic phase). This nematic-to-isotropic transition triggers both bending actuation (Fig. 2c) and mechanical modulation, making it well-suited for applications within the body (Fig. 2d). Similarly, LCEs composed of equivalent substances having a T_{NI} of 35 °C show a wide variation in storage modulus from 1 GPa (at −20 °C) to 0.7 MPa (above 30 °C), demonstrating its temperature-responsive stiffness tunability (Saed et al., 2019).

In another example, Zhang et al. (2020) introduced acrylate group-rich LCEs showcasing robust self-welding between LCE films and reliable thermal actuation. Transitioning from a nematic phase to an isotropic phase upon heating, these LCEs exhibit prominent stiffness modulation and bending actuation. Specifically, the storage modulus dramatically decreases from 1 GPa at −20 °C to below 1 MPa at 80 °C, while maintaining about 10 MPa at body temperature (Fig. 2e). In essence, these LCEs experience a change of over 2 orders of magnitude in storage modulus under temperature conditions similar to the body.

Taken together, LCEs exhibit an ability to reversibly adjust their mechanical properties and demonstrate programmable actuation (i.e., bending, contraction, etc) facilitated by the phase transition between anisotropic and isotropic states in response to external stimuli. Owing to these unique advantages, LCEs can be of use in a wide spectrum of applications, spanning therapeutic soft robots and artificial organ systems (Kim et al., 2022; Liu et al., 2022a).

2.1.3. Liquid metal

Liquid metals emerge as another prospective choice for softening materials in implantable bioelectronics, characterized by their first-order thermodynamic transition between solid and liquid states. This transition triggers abrupt shifts in mechanical and rheological properties by absorbing a large amount of heat at relatively low melting points to rearrange inner atoms (Wang et al., 2022). During phase transitions, the elastic moduli of liquid metals typically vary from a few tens of kPa in liquid states to about 10 GPa when solidified, offering a substantial variation in rigidity. This transition can be induced by various stimuli including thermal, electrical, and magnetic fields. A representative example is gallium (Ga), notable for its biocompatibility (Chen et al., 2023; Chung et al., 2023) and body temperature-triggered phase convertibility, attracting attention in various biomedical applications such as neural probes (Wen et al., 2019; Byun et al., 2019), intravenous needles (Agno et al., 2023), and drug delivery system (Wang et al., 2023). As shown in Fig. 2f (Byun et al., 2021), the mechanically transformative electronic system (TES), constructed with a Ga frame and a soft polymeric encapsulant, showcases stiffness modulation while taking advantage of features in both rigid and soft electronics. Owing to the low melting temperature of 29.8 °C, Ga easily converts to a liquid phase at temperatures of biological tissues (~37 °C). During this transformation, the bending stiffness of the TES changes by 500–5000 times during rigid-to-soft phase conversion, depending on the thickness of the gallium (Fig. 2g). However, TES is challenged with delayed phase transition during freezing due to supercooling issues, which hinder rapid bidirectional stiffness modulation. Accordingly, numerous efforts have been directed toward tackling supercooling problems, including strategies to facilitate heterogeneous nucleation (Byun et al., 2021; Lee et al., 2022a).

Another potential liquid metal of significant interest is eutectic bismuth (Bi)-indium (In)-tin (Sn) based metal alloy, known as Field's metal (FM) (i.e., Bi (32.5 wt%), In (51 wt%), and Sn (16.5 wt%)). Heavy metal-free FM is an emerging liquid metal characterized by its non-toxic nature, low melting point (~62 °C), and large stiffness tuning ability (from negligible modulus to 9.25 GPa) (Hwang et al., 2022; Oh et al., 2023). For example, Hwang et al. (2022) presented a kirigami composite metamaterial sheet comprising an FM frame encapsulated with soft elastomer for a shape and rigidity morphing system. This metamaterial can reversibly tune its stiffness via external thermal stimuli, enabling on-demand 3D shape morphing (Fig. 2h). Despite a relatively high melting point of FM compared to the biological temperature, its biocompatibility (Chen et al., 2023; Nakajima et al., 2008; Rohr, 2002) and exceptional stiffness tunability make it viable for applications such as endoscopes (Zhao et al., 2016), artificial muscles (Liu et al., 2022a) and *in vivo* soft robots (Wang et al., 2023).

However, despite the advantages of nontoxicity and wide stiffness variation, encapsulation is indispensable to ensure the long-term stability of bioelectronics due to concerns regarding the potential leakage of liquid metals in a softened state. To establish sustainable softening bioelectronic interfaces, efforts have been devoted to developing hermetic encapsulation technology to have low permeability of biofluids, and chemical/physical compatibility with biological tissues (Shen et al., 2023). In addition, antimicrobial drugs can be utilized to enhance chemical biocompatibility enabling suppression of chronic inflammatory response (Xu et al., 2023b).

2.1.4. Gel

Gel-sol transition is the phase transition process by which an interconnected network of discrete particles, or solid-like polymeric networks (i.e., gel) transforms into a colloidal suspension (i.e., sol). Various bioactive materials exploiting gel-sol transition mechanisms are recently brought to attention in biomedical applications in the forms of tissue

adhesives (Nishiguchi et al., 2022) and drug delivery systems (Shigemitsu et al., 2020). For instance, Nishiguchi et al. (2022) presented a supramolecular gelatin exhibiting thermally responsive gel-sol transition to regulate the mechanical properties, which can be utilized as a tissue adhesive (Fig. 2i). The reversible gel-sol transition of gelatins depends strongly on their intermolecular hydrogen bonding, where an increase in bonding elevates the gel-sol transition temperature. By functionalizing porcine-derived tendon gelatin (TG) with 2-ureido-4 [1H]-pyrimidinone (UPy) unit (TGUPy), abundant hydrogen bonding is achieved. Accordingly, TGUPy exhibits a higher gel-sol transition temperature of about 40 °C compared to that of TG alone (~37 °C), accompanied by mechanical stability. Through the gel-sol transition responsive to temperature changes, TGUPy showcases a distinct rheological transition with a 200-fold reduction in shear modulus, from approximately 20 kPa at 20 °C to 100 Pa at 40 °C (Fig. 2j).

Unlike thermal stimulation, enzymes and non-enzymatic proteins, including antibodies and membrane receptors, can also act as stimuli to induce gel-sol transition for modulating material stiffness within biological environments. For example, Shigemitsu et al. (2020) developed a non-enzymatic protein-responsive supramolecular hydrogel wherein stiffness is controlled through gel-sol transition. This mechanism involves a combination of protein-responsive enzyme activation and enzyme-triggered gel-sol transition (Fig. 2k). In specific, enzyme-activity triggers (EATs), comprising ligands of a target protein and enzyme (i.e., bovine carbonic anhydrase II (bCAII)) inhibitors, are designed to induce enzyme activation system responsive to the target protein. Upon reaction of EAT with the target protein, steric repulsion leads to the release of bCAII, triggering a gel-sol transition in the hydrogel. The hydrogel exhibits a significant decrease in storage modulus from 2300 Pa to 770 Pa upon the addition of bCAII (Fig. 2l). Changing the type of protein ligand further adds diversity to its responses to different non-enzymatic proteins. Therefore, a gel-sol transition mechanism can be designed depending on the protein types, which can selectively modulate the material stiffness in a specific body environment.

The gel-sol transition mechanism is distinctive for its biocompatible stimuli conditions (e.g., low transition temperature, enzymes, and biofluid). While it may not exhibit as extensive stiffness changes compared to other PTSMs, its ability to finely tune stiffness makes gels a compelling option for drug delivery applications by controlling drug adsorption and release through their adjustable mechanical properties. Moreover, ongoing research into the gel-sol transition mechanism aims to enhance bioactivity and refine the controllable stiffness-tuning ability, paving the way for optimal softening biomaterials in tissue engineering (Park et al., 2023).

2.2. Softening materials based on molecular conversion mechanism

Molecular conversion-based softening materials (MCSM) are promising candidates to implement stiffness-tuning functionality, relying on either their physical supramolecular interactions or chemically reversible covalent bonds. Interaction between polymer networks changes in response to external stimuli, such as temperature change, biofluid, and pH, inducing dissociation and recombination of cross-linked bonds for the stiffness tuning of softening materials.

MCSMs utilizing supramolecular interactions rely on non-covalent bonds (i.e., secondary interaction), such as metal-ligand coordination (Lai et al., 2018; Wang et al., 2020a), hydrogen bonding (Hu et al., 2016; Zhou et al., 2022; Asakura et al., 2017; Dagnon et al., 2012), and host-guest interactions (Han et al., 2012), to achieve variable stiffness features. For example, softening polymers utilizing metal-ligand interaction as a stiffness-tuning strategy have been reported (Lai et al., 2018; Wang et al., 2020a). Lai et al. (2018) reported a thermodynamically softening polymer, PDMS–COO–Zn, which utilizes Zn(II)-carboxylate coordination as a dominant cross-linking site (Fig. 3a). According to hard and soft acids and bases (HSAB) theory, PDMS–COO–Zn exhibits high rigidity (elastic modulus of 480 MPa) at room temperature (~25 °C) due to the strong Zn(II)-carboxylate bonding, surpassing the strength of hydrogen bonding. With temperature sensitivity inherent in the coordination equilibrium, PDMS–COO–Zn softens and becomes viscoelastic when exposed to heat (storage modulus of 0.06 MPa at 125 °C), and the bonds dissociate at the cross-linking equilibrium state (Fig. 3a, left and right). PDMS–COO–Zn softened at a temperature above 50 °C can withstand strains up to 50% due to increased PDMS-COO^- chain mobility. This capability surpasses that of rigid polymers, which are typically limited to a 4% strain at room temperature (Fig. 3a, middle).

On the other hand, MCSMs with chemically reversible covalent bonds allow stiffness tuning through the dynamic coupling and decoupling of covalent bonds. Notably, various reactions such as the Diels-Alder reaction (Hu et al., 2015; Kuang et al., 2021), Schiff base linkages (Deng et al., 2022a), Urea exchange reaction (Chen et al., 2020), and disulfide exchange reaction (Zhang et al., 2018b, 2023a) provide versatile platforms for achieving this tunability. For instance, Reeder et al. (2014) proposed a dynamic covalent material in the form of a softening organic thin film transistor (OTFT). Fabricated on a thiol-ene/acrylate SMP substrate, this technology harnesses the merits of both rigid and soft implantable bioelectronics owing to its inherent softening properties. Thiol-ene/acrylate polymer (Ware et al., 2012b, 2014; Simon et al., 2017; Do et al., 2017) contain cross-linked networks generated by the reaction of thiol and ene functional groups, forming a robust three-dimensional network. The introduction of the acrylate monomer further contributes to the development of a robust cross-linking network, attributed to its excellent thermomechanical properties that result in a densely interconnected structure (Xu et al., 2012). An increased temperature promotes molecular mobility within the network, which softens the materials by reducing their overall stiffness. The shear modulus of the substrate was approximately 80 MPa at 37 °C in fluid conditions, similar to an *in vivo* environment, and 600 MPa at 25 °C in dry conditions.

In contrast to typical MCSMs that rely on a single bonding type, a new class of MCSMs incorporating multiple bonding types has been explored. Zhang et al. (2018b) presented a poly (thioctic acid (TA)) based supramolecular polymeric material that uses 1,3-diisopropenylbenzene (DIB) and iron (III) ions to enhance the thermodynamic stability. The resulting supramolecular polymer network, poly (TA-DIB-Fe), utilizes three different types of dynamic chemical bonds: (i) dynamic covalent disulfide bonds, (ii) noncovalent hydrogen bonds, and (iii) iron (III)-carboxylate coordinative bonds. These dynamic bonds modulate the rigidity of the supramolecular copolymer in response to temperature. Particularly, heat-labile H-bonds and covalent disulfide bonds significantly contribute to the relaxation of the entire polymer network with thermal stimuli, which softens the supramolecular polymer.

Unlike MCSMs regulating their stiffness by thermal stimuli, pH can also serve as a catalyst to adjust the rigidity of softening materials. For example, Kim et al. (2016) fabricated pH-responsive stiffness tunable polyelectrolyte microcapsules consisting of poly (acrylic acid) (PAA) and branched poly (ethylenimine) (bPEI) through nanoscale interfacial complexation in emulsion (NICE) method. To create a microcapsule structure using the NICE approach, two polymers, PAA and bPEI, should be complexed to generate the insoluble nanolayer at the inner water (W)/oil (O) interface of a W/O/W double emulsion. As the pH of surroundings rises from 2 to 6, the elastic modulus of (PAA/bPEI) NICE microcapsules decreases by more than two orders of magnitude. For this reason, polyelectrolyte networks get loose and generate pores as pH increases. Likewise, diverse pH-responsive MCMSs, such as poly (vinylpyrrolidone)/poly (methacrylic acid) (PVPON/PMMA) (Elsner et al., 2006), Alginate-glycidyl methacrylate (Alg-GMA) (Lima et al., 2018), O-carboxymethyl chitosan (CMCS) based hydrogel (Yu et al., 2021), glutamic acid grafted chitosan (CH-g-SA) hydrogel (Nisar et al., 2021), β-cyclodextrin-diethylenetriamine (β-CD-DETA) based polymers

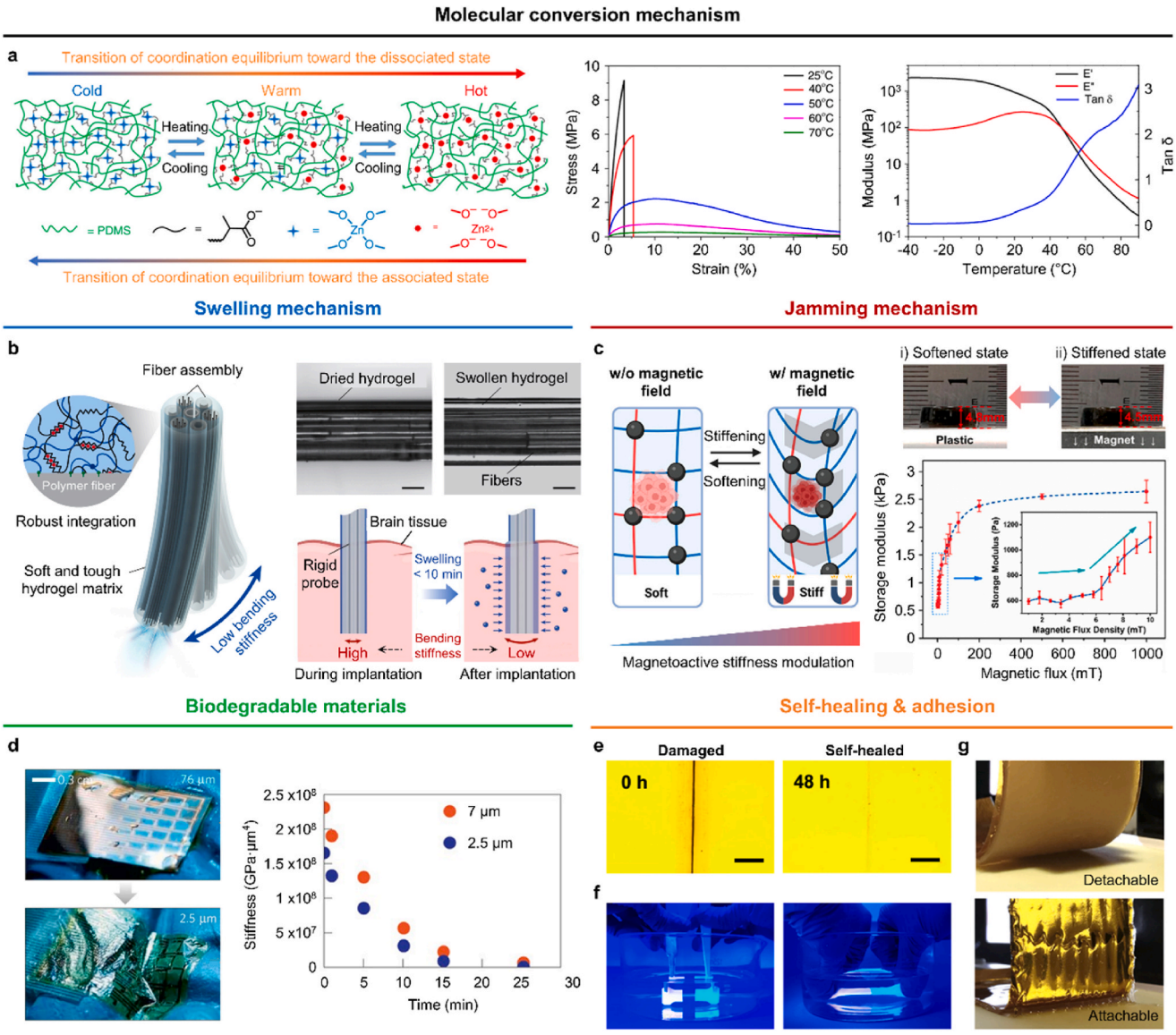

Fig. 3. Softening materials through molecular conversion mechanisms and diverse softening approaches complying with *in vivo* conditions. a) Molecular conversion-based softening material that modulates the rigidity by alterations in dynamic bonds. Schematic diagram (left) showing the polymeric network transition of metal-ligand interactions, which is a type of dynamic noncovalent interaction, in response to temperature changes. Stress-strain curves of PDMS–COO–Zn polymer at different temperatures (middle). Temperature-dependent storage modulus (E'), loss modulus (E''), and tan δ of PDMS–COO–Zn polymer (right) (Lai et al., 2018) (Copyright, 2018; Springer Nature). b) Softening approach by the hydration of hydrogel network based on swelling behavior. Schematic illustration of a hydrogel-based hybrid probe highlighting the potential of the hydration softening method (left). Optical microscope images of the hybrid probe with fully swollen and dehydrated hydrogel matrix (top right). Conceptual illustration of the softening mechanism based on hydrogel swelling through water absorption in the tissue (bottom right) (Park et al., 2021) (Copyright, 2021; Springer Nature). c) Softening approach by enzyme responsive gel-sol transition provoked by enzyme activation system using non-enzymatic protein. Schematic illustration depicting reversible gel-sol transition of supramolecular hydrogel composite triggered by non-enzymatic protein (top left). Rheological properties of the hydrogel in response to the enzyme (i.e., bovine carbonic anhydrase II, bCAII) (top right). Schematic of non-enzymatic protein-activated softening mechanism including sequential reactions; (i) protein-triggered enzyme activation and (ii) enzyme-sensitive gel-sol transition (bottom). Enzyme-activity trigger (EAT) which releases previously inhibited bCAII in response to a specific non-enzymatic protein and supramolecular hydrogel undergoing a gel-sol transition triggered by the released bCAII (Shigemitsu et al., 2020) (Copyright, 2020; Springer Nature). d) Softening approach by pH-responsive stiffness modulation. Schematic presenting Nanoscale Interfacial Complexation in Emulsion (NICE) method to form polyelectrolyte microcapsules, which undergo a stiffness change in response to pH variations (top left). Optical microscope images of polyelectrolyte microcapsules under different pH conditions (i.e., pH 2 and pH 6) showing negligible pH effect on the shape of microcapsules (bottom left). Elastic moduli at varied pH conditions of the microcapsule (right) (Kim et al., 2016) (Copyright, 2016; American Chemical Society). e) Softening approach by reconfiguration of the dynamic magnetoactive polymer under a magnetic field. Schematic illustration (left) presenting the reversible rigidity modulation principle of magnetic microparticle-hydrogel network depending on the magnetic field. Storage moduli of the magnetic hydrogel as a function of magnetic flux density (right) (Shou et al., 2023) (Copyright, 2023; American Chemical Society). f) Structural softening approach enabled through the dissolution of biodegradable support materials. Optical images of neural electrode arrays integrated with a biodegradable silk fibroin supporter establishing a conformal contact with a brain model (left). Time-dependent change in the bending stiffness of a silk fibroin film during dissolution (right) (Kim et al., 2010) (Copyright, 2010; Springer Nature). g) Self-healable polymers. Photographs of self-healable polymers in a damaged state (left) and recovered state (right) depicting self-healing properties induced by the softening mechanism. Photographs demonstrating the underwater self-healing behavior regardless of the environment (bottom) (Liu et al., 2022b) (Copyright, 2022; Springer Nature). h) Optical images illustrating reversible debonding-on-demand adhesives triggered by thermal stimuli (top: stiff and non-adhesive at 20 °C, bottom: soft and adhesive at 32 °C) (Gao et al., 2021) (Copyright, 2021; Elsevier).

(Han et al., 2012), and so on (Yoshikawa et al., 2011), show a broad range of stiffness induced by pH-responsive molecular reconstruction. Since each region of the body possesses a variety of pH concentrations (e.g., pH 7.35 to 7.45 in the blood, pH 1.5 to 3.5 in the stomach), stiffness can be adjusted with the change in biological surroundings.

Compared to the phase transition-based softening mechanism from a kinetic perspective, MCSMs regulate their inherent mechanical properties with dynamic dissociation and recombination of molecular bonds. Owing to the reversible molecular bonding reconfiguration, MCSMs can also obtain self-healing and bio-adhesive properties to improve the functionality and versatility of softening materials. Such multifunctional properties of softening materials will be mentioned in section 2.6 in detail.

2.3. Softening materials based on swelling mechanism

Among various types of softening approaches, swelling can be used to adjust the mechanical behavior of polymers through water absorption due to plentiful water content (e.g., biofluids) within the human body. As a prime example, hydrogels are generically referred to as a cross-linked polymer network with a substantial water content. With hydrophilic functional groups along their polymer chains, hydrogels exhibit a strong affinity to water, facilitating extensive water absorption within the network. The entire polymer network substantially expands by water absorption, as the entrapped water molecules engage in hydrogen bonding and electrostatic interactions with hydrogels for water retention. Chemically cross-linked networks loosely hold the hydrogel structure even after swelling, thanks to enhanced chain mobility within the network. Accordingly, the water content in hydrogels becomes pivotal in precisely modulating their stiffness through hydration or dehydration (Xu et al., 2023a; Zhang et al., 2018a).

Numerous studies on hydrogels that can tune their mechanical stiffness by hydration and dehydration, have broadened their applications in implantable bioelectronics. For instance, Park et al. (2021) presented a hybrid multifunctional neural probe encapsulated by poly (acrylamide)-alginate (PAAm-Alg). PAAm-Alg is a hydrogel with high biocompatibility and exceptional chemical reliability under physiological conditions, alongside a chemo-mechanical resemblance to biological tissue (Fig. 3b, left). While the inherent softness of PAAm-Alg poses insertion challenges for neural probes into the deep brain regions, a dehydrated hydrogel with a high bending stiffness of approximately 2.6 N/m facilitates brain tissue penetration. After implantation, the dried hydrogel converts to a soft, swollen state, showing bending stiffness lowered to about 0.42 N/m through water diffusion (Fig. 3b, top right and bottom right). Various swellable materials, such as poly (vinyl alcohol) (PVA) (Butylina et al., 2016), alginate (Lee et al., 2000), poly (ethylene glycol) diacrylate-alginate (PEGDA-Alg) (Nurlidar et al., 2023), poly (2-hydroxyethyl methacrylate) (pHEMA) (Opdahl et al., 2003; Zare et al., 2021; Wichterle and Lím, 1960), and poly (styrene)--*block*-poly (acrylic acid) (PS-*b*-PAA) block copolymer (Yang et al., 2013), can also leverage water swelling mechanism for softening.

The biggest advantage of the swelling mechanism is the immediate and spontaneous softening upon implantation, eliminating the need for additional equipment to exert stimuli. Furthermore, hydrogels possess tissue-like mechanical properties when swollen and exhibit excellent chemical biocompatibility, making them ideal for biomedical applications (Yuk et al., 2022). In recent decades, hydrogels with high fracture toughness have been developed to enhance the robustness and reliable functionality enabling long-term stability (Sun et al., 2012; Zhou et al., 2023). Ultimately, swelling-based softening materials, specifically hydrogels, enable the development of various implantable applications (e.g., neural probes and implantable microneedles) due to their fascinating physicochemical properties and bio-intimacy.

2.4. Softening materials based on jamming mechanism

The jamming mechanism is one of the well-known stiffness-tuning strategies and is applicable to composites with small additives (i.e., particles, granules, layers, etc) embedded within the matrix. External stimuli such as pneumatic pressure and magnetic field trigger the jamming structures, as internal additives are forced to tightly contact and attract each other, inducing an increase in stiffness. On the contrary, the internal constituents can freely rearrange their structure without mechanical coupling inducing an unjammed state (i.e., softened state with low stiffness) through the removal of external stimuli. Depending on the existence of stimuli, rigidity can be reversibly controlled by the dynamic reconfiguration of additives inside the jamming structure.

To incorporate jamming-based softening strategies into implantable devices, careful selection of stimuli for stiffness modulation is vital. Magnetic field holds a great potential due to its unparalleled ability to penetrate biological tissues under *in vivo* environments (Rotundo et al., 2022). In general, biological tissues typically lack magnetic properties, which enable them to manifest non-invasive magnetic effects within the body without field attenuation (Kim and Zhao, 2022). Owing to these advantages, extensive research has explored the use of a magnetic field for jamming-based stiffness modulation. For example, Shou et al. (2023) reported a magnetoactive hydrogel containing magnetic microparticles (MMPs) within a gelatin/hyaluronic acid matrix, capable of reversible magneto-induced stiffening and softening (Fig. 3c, left). Under a magnetic field, MMPs tightly grafted to a hydrogel matrix align and get attracted along the magnetic field. Accordingly, the entire hydrogel matrix undergoes the macroscopic contraction following the dynamic mobility of MMPs, which brings about strain-induced stiffening. Conversely, the stiffened magnetic hydrogel can revert to a soft state by eliminating an external magnetic field (Fig. 3c, top right). For the softening process, the attracted MMPs return to initial sites, enabling a relaxed polymeric network. Utilizing this softening strategy, the magnetic hydrogel constructed by GelGMA/HAGMA (10:1) hydrogel with 2% MMPs exhibits about 78.8% decrease in storage modulus, specifically changes from ~2640 Pa (at 1 T magnetic field) to ~560 Pa (without magnetic field) (Fig. 3c, bottom right).

The jamming mechanism provides a fast and reversible stiffness modulation with simple operational methods. However, several challenges hinder its seamless integration into implantable bioelectronics. First, the jamming technology favors stiffening over softening effects, posing a hurdle in achieving design flexibility. Second, it requires substantial apparatus to apply external stimuli, thereby limiting its application to diverse implantable devices. To overcome these restrictions, recent studies are actively exploring solutions, targeting its use as an *in vivo* surgical soft robot (Gaeta L. J et al., 2023; Cianchetti et al., 2013), and drug screening platform (Shou et al., 2023). Furthermore, the inner constituents are being potentially designed with biomaterials to enhance the biocompatibility of the overall jamming system, which makes it promising for various biomedical fields (Riley et al., 2019).

2.5. Softening strategies using biodegradable materials

Considering the structural design of devices, achieving softening in bioelectronics can also be accomplished through the integration of biodegradable sacrificial layers. These materials, undergoing chemical or biological decomposition via enzymatic processes under physiological conditions, play a pivotal role in this softening approach. To design the softening implantable device, a biodegradable material layer is incorporated into the ultrasoft bioelectronics device, which lacks mechanical robustness for standalone implantation. Outside of the body, the biodegradable layer exhibits robust mechanical properties to mechanically support the entire bioelectronics. However, upon implantation, the biodegradable materials dissolve, leaving behind only the soft components of the device. This approach provides a straightforward softening effect by incorporating biodegradable materials with existing

soft bioelectronics.

Biodegradable materials are classified into natural and synthetic biomaterials, retrieved from either natural sources or chemical manufacturing, respectively. Common biodegradable materials from natural sources include silk fibroin, polysaccharides (Deng et al., 2022b), and plant-based cellulose (Sarkar et al., 2023; Sannino et al., 2009). Notably, silk fibroin is biocompatible as it decomposes through water and proteolytic enzymes in the body, making it a favored choice in biomedical applications (Arai et al., 2004; Cao and Wang, 2009). As shown in Fig. 3d–a softening neural electrode device integrates ultrathin polyimide (PI) based bioelectronics on a silk fibroin layer, achieving seamless integration with the brain as the silk fibroin dissolves in biofluids (Fig. 3d, left) (Kim et al., 2010). Neural devices with 2.5 and 7 μm-thick PI-based bioelectronics on top of about 25 μm-thick silk fibrin substrate, respectively show a remarkable decrease in bending stiffness in water at body temperature (Fig. 3d, right). Similarly, silk fibroin serves as a biodegradable sacrificial substrate for parylene-C based ultrathin neural probes, enabling brain tissue insertion and softening effects (Cointe et al., 2022). Aside from silk fibroin, various biodegradable synthetic polymeric materials including polylactic acid (PLA) (Luckachan and Pillai, 2011), poly (lactic-*co*-glycolic acid) (PLGA) (Shah and Vasava, 2019), and poly (caprolactone) (PCL) (Archer et al., 2023) can be utilized as substrates in implantable bioelectronics. Beyond polymers, non-polymeric biodegradable materials, such as Mg alloy (Zhang et al., 2023c; Hwang et al., 2015), SiO_2, spin-on-glass (SOG) (Hosseini et al., 2021; Kang et al., 2015; Doucet and Carlotti, 1994), and poly (4-hydroxybutyrate) (P4HB) (Keridou et al., 2020) offer promise as encapsulating layers, insulators, and dielectric layers in softening bioelectronics.

2.6. Softening materials with multifunctionality

Materials discussed in previous sections (2.1–2.5) mainly focus on various stiffness-tuning mechanisms. This section discusses their additional functionalities, such as self-healing properties and bio-adhesion, achievable through the softening process. These functions transcend conventional bioelectronics, as they impart multifunctionality beyond a mere improvement in mechanical adaptability and biocompatibility.

The self-healing property, the ability to restore physically damaged materials to their original state, possesses a crucial role in implantable bioelectronics (Wang and Urban, 2020). Most implantable devices are challenging to routinely inspect and manage, requiring secondary surgery to recover from inevitable damage or functional failure. Given such challenges, self-healing ability provides beneficial features to implantable devices enabling not only structural and functional restorations but also mechanical robustness for long-term reliability. To derive the self-healing ability from the softening procedure, dynamic covalent and non-covalent bonding as mentioned earlier (section 2.2) are significant to leverage the dynamic equilibrium of the cross-linking network. Such bonding brings about self-healing properties as well as stiffness modulation through reversible dissociation and recombination of polymer chains (Fig. 3e). As shown in Fig. 3f, Liu et al. (2022b) presented a luminescent fluorine elastomer with perovskite quantum dots (TFE–HF–QD) exhibiting self-healing properties derived from large amounts of ion–dipole and dipole–dipole interactions. The core factor of self-healing ability for TFE–HF–QD is the dipole-dipole interaction, which can also affect stiffness modulation through reversible control over the chain mobility. Besides, dynamic bonding such as a reversible covalent bond (Zhang et al., 2018b; Choi et al., 2022), metal-ligand interaction (Lai et al., 2018; Wang et al., 2020a), and hydrogen bonding (Yu et al., 2021; Zhao et al., 2017a) can arouse both self-healing and stiffness tuning abilities.

Another prospective functionality of softening materials is bio-adhesion. The bio-adhesive property can be used to form conformable tissue–device interfaces, improving physiological signal sensing, drug delivery, and long-term reliability. While bio-adhesion has been investigated for designs such as octopus suckers (Chen and Yang, 2017), gecko-inspired structures (Acharya et al., 2023), and Velcro (Ahn et al., 2013)), it can be also induced by the chemical and physical reactions at the tissue-device interface, with examples including phase transition (Gao et al., 2021), hydrogen bonding (Zhang et al., 2018b), and so on (Yang et al., 2013; Lai et al., 2018). For example, Gao et al. (2021) proposed the bistable adhesive polymer (BAP) showing reversible bonding and debonding features with stiffness modulation through a phase transition mechanism (Fig. 3g). At a high temperature above 32 °C, the semicrystalline alkyl side chains of BAP convert into an amorphous state with higher flowability. This phase change significantly enhances its adhesive properties, with a rise in peel strength between BAP film and artificial skin to about 45.7 N/m at 32 °C in the amorphous state, which is a substantial increase from the 3 N/m observed in its semicrystalline state at room temperature. In addition to chemical reaction, Yang et al. (2013) presented an adhesion method using swellable materials for mechanical interlocking within biological tissues. Once inserted into biological tissues, the swellable material expands substantially by absorbing surrounding biofluid, tightly grafting into the tissue with a 3.5-fold increase in adhesion strength alongside a water-swelling induced softening effect.

Recently, numerous implantable bio-integrated systems, showcasing self-healing and bio-adhesive features, have demonstrated their superiority in diverse biomedical fields, including self-healable neural devices (Song et al., 2020), tissue-adhesive bioelectronics (Deng et al., 2021; Choi et al., 2023), and drug delivery systems (Shaikh et al., 2011). Such multifunctionality can yield synergistic effects on softening bioelectronics, which only offer mechanical benefits. This includes enabling sutureless interfacing, enhancing physiological signal recording, and ensuring long-term reliability of device performance beyond mechanical softening.

3. Application for softening implantable bioelectronics

Utilizing softening materials greatly enhances the versatility and functionality of implantable bioelectronics. The initial rigidity aids easy implantation, while post-implantation softness minimizes tissue wounds and improves adaptability. This section delves into two main applications: (i) tissue-penetrating bioelectronics and (ii) tissue-conformal bioelectronics.

3.1. Softening implantable bioelectronics for tissue penetration

Conventional rigid electronics, capable of penetrating body tissues, often cause extensive tissue damage and inflammation due to mechanical mismatches within the body. In contrast, softening implantable bioelectronics, designed to reduce modulus post-penetration, offer mechanical compatibility that minimizes tissue damage. Crucial for delicate regions such as the brain, the heart, and bowel, their flexibility ensures safe and effective interaction while minimizing harm.

A key application of penetrating softening bioelectronics is in neural probes for brain tissue injection. These probes soften after penetration, triggered either by body temperature (Byun et al., 2019; Ziemba et al., 2023; Ware et al., 2012a, 2014) or biofluids (Zhou et al., 2022; Park et al., 2021; Hess-Dunning and Tyler, 2018). For example, a liquid metal-based neural probe developed for chronic *in vivo* optogenetics, shown in Fig. 4a, changes its stiffness in response to the body temperature (Byun et al., 2019). Upon penetrating brain tissue, the 50 μm-thick gallium layer undergoes a significant modulus shift from 50 MPa to 30 kPa (~99.9% decrease). This distinctive behavior is attributed to the low melting point of gallium (29.8 °C) that provides rigidity at room temperature (~25 °C) for deep brain penetration and softening near body temperature (~37 °C), enhancing biomechanical compatibility with brain tissue. This softening effect reduces inflammatory glial responses and lesion sizes compared to rigid tungsten probes, as illustrated in Fig. 4b. Another body temperature-responsive approach involves

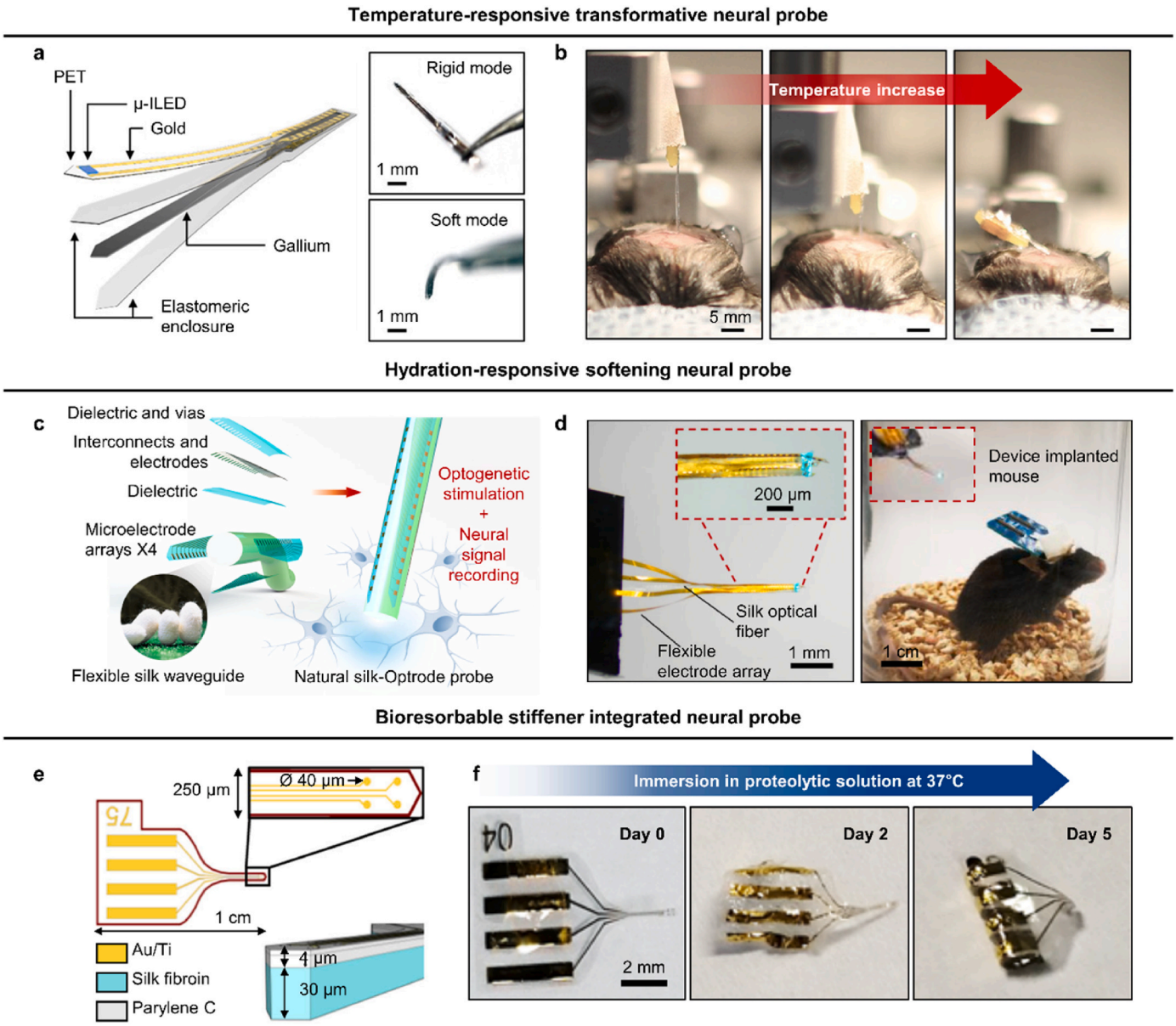

Fig. 4. Softening implantable bioelectronics for tissue penetration. (a–b) Temperature-responsive transformative neural probe. a) Conceptual illustration (left) and optical images (right) of a stiffness-tunable liquid metal-based neural probe. Gallium needle encapsulated with silicone (e.g., Ecoflex) is placed under the flexible optogenetic probe. Due to a low melting temperature of gallium (29.8 °C), the transformative neural probe becomes rigid at room temperature (~25 °C; top right) and softens at temperature near body temperature (~37 °C; bottom right). b) Photographs of stiffness-tunable neural probe gradually being injected into the deep brain. Gallium-based neural probe is sufficiently rigid outside the body to penetrate the brain tissue (left and middle), while it softens inside the body due to body temperature (right), ensuring biomechanical compatibility with the brain tissue with reduced lesion size and inflammatory glial responses (Byun et al., 2019) (Copyright, 2019; AAAS). (c–d) Hydration-responsive softening neural probe. c) Schematic of a hydration-responsive silk-based optical fiber integrated with flexible multichannel electrode arrays for simultaneous optogenetic stimulation and electrophysiological recording. Exposure to biofluid after implantation causes the disruption of hydrogen bonds in the silk comprising the optical fiber, leading to a significant decrease in Young's modulus from 38.7 MPa to 3.53 MPa. d) Photographs of silk optical fiber connected to laser equipment (left) and implanted into the brain of a freely moving mouse (right). When implanted *in vivo*, the flexible silk optical fiber gradually softens, exhibiting reduced mechanical stiffness with less immunoreactive glial responses and tissue lesions (Zhou et al., 2022) (Copyright, 2022; Springer Nature). (e–f) Bioresorbable stiffener integrated neural probe. e) Schematic illustration of an immersion-triggered bioresorbable silk-parylene bilayer probe capable of various types of neural recording (e.g., local field potential (LFP), multi- and single-unit spike recording). High initial Young's modulus of biodegradable silk layer (~3 GPa) supports the implantation of an ultrathin flexible parylene-based probe into deep brain tissue, and this silk fibroin-based layer can be dissolved by solution-containing enzymes (e.g., biofluid). f) Optical images of the silk fibroin layer of the probe dissolving over time in enzyme-contained PBS at 37 °C. The probe has become extremely soft, which is expected to achieve better compliance with surrounding tissues while minimizing rejection when implanted in the brain (Cointe et al., 2022) (Copyright, 2022; Springer Nature).

polymers transitioning from a glassy to a rubbery state at their T_g (Ziemba et al., 2023; Ware et al., 2012a, 2014), such as the thiol-epoxy/maleimide ternary networks. Used in softening intracortical microelectrode arrays, these polymeric probes shift their modulus from over 1 GPa down to 30 MPa through glass transition in physiological environments, affirming their potential in softening bioelectronic applications (Reit et al., 2016).

Biofluid-triggered devices, extensively studied in the field, make use of materials such as silk (Zhou et al., 2022), hydrogels (Park et al., 2021), and nanocomposites (Harris et al., 2011; Nguyen et al., 2014;

Hess et al., 2011; Hess-Dunning and Tyler, 2018). Silk-based optical fiber probes with flexible 128 recording channels adjust their stiffness post-implantation. These probes demonstrate efficient electrophysiological recording capabilities during intracranial light stimulation, with minimal optical losses and reduced glial responses post-surgery (Fig. 4c) (Zhou et al., 2022). Upon implantation into a mouse brain (Fig. 4d), the flexible silk optical fibers gradual soften as biofluid breaks the hydrogen bonds in the silk, reducing Young's modulus of the fibers by ~90.9% (38.7 MPa–3.53 MPa). Similar to silk optical fiber, PAAm-Alg hydrogel probes (Park et al., 2021) and nanocomposite microprobes, inspired by the sea cucumber dermis (Harris et al., 2011), also exhibit effective penetration and rapid compliance with cortical tissue, enabling stable, long-term neural recording with minimized glial scar. Beyond the design based on softening the device structure itself, some neural probes utilize biodegradable sacrificial layers as part of their softening mechanism (Cointe et al., 2022). Illustrated in Fig. 4e is a biodegradable sacrificial layer composed of immersion-triggered biodegradable silk fibroin, which temporarily enhances probe's rigidity, aiding in its injection into neural tissue. Subsequent to implantation, the gradual degradation of silk fibroin layer allows the probe to achieve dynamic tissue-adaptation, facilitating chronic neural recordings. Silk fibroin stands out as an exceptional supporting material owing to its biocompatibility and biodegradability at body temperature. Furthermore, its high initial Young's modulus (E ~3 GPa) facilitates the implantation of an ultrathin parylene-based probe into deep brain tissue. Following implantation, the silk fibroin layer dissolves in enzyme-containing solution (i.e., biofluid), making the remaining probe parts extremely soft. These processes, detailed in Fig. 4f, demonstrate the improved compliance of softened implantable probe with surrounding brain tissues, along with reduced rejection risks during brain implantation.

Beyond neural applications, softening penetrable bioelectronics can be employed for various biological tissues and organs (Sun et al., 2022). Electrodes utilizing magnetic liquid metal (e.g., liquid metal incorporated with Fe_3O_4 nanoparticles) demonstrate remarkable stiffness tunability spanning five orders of magnitude, aiding insertion and post-insertion flexibility in soft tumor-affected tissues without interfering with normal activity. Responsive to alternating magnetic fields, these electrodes can generate inductive heat, efficiently impeding tumor growth and extending survival times. Similarly, drug-containing PVA hydrogels are used for the treatment of diabetic ulcers (Zhang et al., 2023b). The mechanical strength of PVA hydrogels is dynamically modulated through ionic interactions – sulfate ions enhance rigidity to facilitate initial penetration, while nitrate ions soften the PVA hydrogels, enabling adaptation to wounds and sustained drug release. The integration of adjustable stiffness and treatment within a single softening electrode offers a minimally invasive approach to disease treatment, preserving adjacent biological tissues.

3.2. Softening implantable bioelectronics for tissue-conformal operation

Stimuli-responsive softening materials are also crucial for tissue-conformal operations in implantable bioelectronics. Typical soft electronics conform to body curvatures, but they face limitations in withstanding high contact forces and ensuring easy handling. Softening bioelectronics overcome these challenges. They achieve this through an ingenious mechanism involving initial rigidity for shape maintenance, followed by softening for adaptation to complex 3D surfaces of organs (e.g., brain and heart) or cylindrical tissues (e.g., nerve and spinal cord). This innovative softening approach not only minimizes mechanical mismatches during implantation but also enhances functional interactions with tissues, including sensing, recording, and stimulation.

One major application involves interfacing complex biosurfaces for efficient electrocorticography (ECoG) and electrocardiogram (ECG) sensing. Synthesized through the polymerization of polycaprolactone diol, poly (hexamethylene diisocyanate), and hexamethylene diisocyanate (Jiao et al., 2023), SMPs exhibit a remarkable softening property, transitioning from a modulus of 100 MPa–700 kPa (i.e., 99.3% decrease) near body temperature (~38 °C). This characteristic facilitates the fabrication of multi-layered devices in a rigid state and ensures firm contact with intricate biosurfaces when in a soft state. Consequently, it markedly enhances the precision of ECoG recording for epilepsy tracking and ECG recording for cardiac health monitoring. Integrating biodegradable supporters is an approach for attaining conformal contact with tissues. As mentioned in section 3.1, silk fibroin, known for its biocompatibility and biodegradability, is also widely used as the supporter in implantable bioelectronics designed for tissue-conformal operation (Kim et al., 2010; Shi et al., 2019). Fig. 5a–c illustrate an example of implantable multifunctional bioelectronics with a bottom substrate made of silk fibroin (Shi et al., 2019). As the silk substrate gradually dissolves in biofluids, capillary forces at the interface of the brain tissue and the thin electronics layer enable the device to conformally mount on the brain tissue, thereby substantially enhancing the quality of ECoG recordings (Fig. 5b and c). To expand the application of silk fibroin beyond its role as a bio-dissolvable substrate, Shi et al., (2019) broadened its functionality by incorporating drugs within the silk fibroin matrix. This facilitates in situ drug delivery while silk substrate dissolves, contributing to the softening of the device (Shi et al., 2019).

Another application involves seamless wrapping of implantable bioelectronics around cylindrical structures, such as nerves or the spinal cord, for precise stimulation or neural recording. Thiol-ene/acrylate-based polymer has been widely used for this application due to its exceptional softening at body temperature (~37 °C) (Ware et al., 2012b; González-González et al., 2018), as exemplified in Fig. 5d–f. Fig. 5d shows temperature-responsive softening nerve cuffs with thin film multi-electrodes supported by a thiol-ene/acrylate SMP substrate, designed for selective neuromodulation and precise neural recording (González-González et al., 2018). When exposed to a biofluid-mimicking environment (e.g., 37 °C PBS), the storage modulus of the thiol-ene/acrylate substrate of this device drastically decreased from 2380 MPa to 550 MPa (a ~77% decrease) within 30 min (Fig. 5e). This softening capability, as depicted in Fig. 5f, ensures a secure wrapping of cuffs around various nerve types (Ware et al., 2012b; González-González et al., 2018) and spinal cords (Garcia-Sandoval et al., 2018) within the body, all of which are cylindrical structures. This feature ensures effective electrical stimulation and neural recording. Meanwhile, ester-free SMPs (e.g., thiol-ene) have been further investigated to boost the stability of SMP-based substrates. This material retains its mass and shape for 24 months after softening in an *in vivo* environment (i.e., temperature of 37 °C with humidity), ensuring prolonged functionality of bioelectronics made from this material and consequently extending the lifespan of the device within the body (Garcia-Sandoval et al., 2021).

4. Current challenges and future directions in softening implantable bioelectronics

Softening implantable bioelectronics, designed to adjust their rigidity in response to external stimuli, combine the merits of both rigid and soft devices: the initial rigid state offers portability and easy tissue penetration, while the subsequent softened state ensures biocompatibility and a robust functional interface with biological tissues. Widely studied external stimuli include temperature, moisture, magnetic fields, biological triggers (e.g., enzymes and proteins), or the combination of these. These ongoing advancements in designs and stimulation strategies for stimuli-responsive materials amplify the versatility and efficiency of these bioelectronics, extending to applications in tissue-penetrating and tissue-conformal implants. However, further breakthroughs remain imperative to unlock their full potential. The ideal softening implantable bioelectronics should encompass four key features: a) bidirectional transformation, b) a transformative electro-mechanical all-in-one platform, c) controlled *in vivo* transformability, and d) a residue-free or biodegradable implant, as illustrated in Fig. 6.

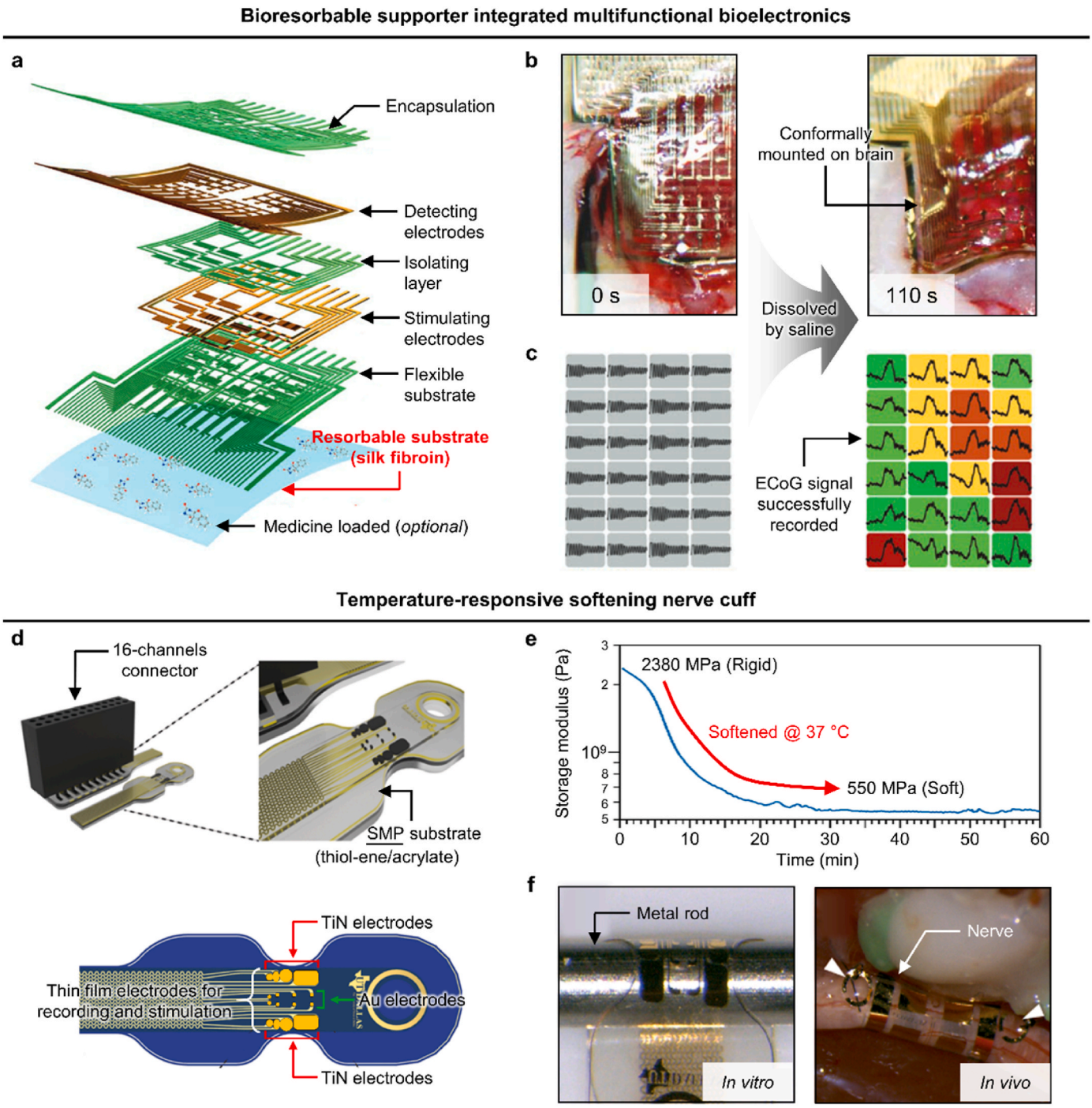

Fig. 5. Softening implantable bioelectronics for tissue-conformal operation. (a–c) Bioresorbable supporter integrated multifunctional bioelectronics. a) Exploded view of silk-supported soft bioelectronics capable of conformal brain integration for electrocorticography (ECoG) recording. The bottom of the device is composed of a resorbable substrate made of silk fibroin, which gradually dissolves when exposed to water (e.g., biofluid). Medicine can be loaded within the bottom substrate, if necessary, and released for drug delivery while being dissolved. Device images (b) and ECoG signals (c) acquired before (left) and after (right) the dissolution of silk fibroin substrate. Dissolution of the bottom substrate of the device improves the conformal contact of microelectrodes on the highly convoluted surfaces of a rat brain, thereby improving ECoG recording quality. Here, saline water was poured to promote the dissolution (Shi et al., 2019) (Copyright, 2019; Wiley). (d–f) Temperature-responsive softening nerve cuff. d) Schematic illustrations of thin film multi-electrode softening nerve cuffs for selective neuromodulation and neural recording. Schematics (top and bottom) show the structure and electrode configuration of the device, respectively. There are a total of 16 channel electrodes, among which 8 are made of titanium nitride (TiN), and the other 8 are made of gold (Au). Substrate of the device is made of thiol-ene/acrylate-based SMP, which softens at body temperature (~37 °C). e) Storage moduli of SMP over time after soaking in PBS at 37 °C. Modulus has been significantly decreased from 2380 MPa to 550 MPa in 30 min, allowing the overall substrate to be softened. f) Optical images of multi-electrode softening cuffs wrapped tightly around the metal rod (left) and superior cluneal nerve (right) after being softened. Conformal contact on cylindrical shaped-nerve allows efficient electrical stimulation and neural recording (González-González et al., 2018) (Copyright, 2018; Springer Nature).

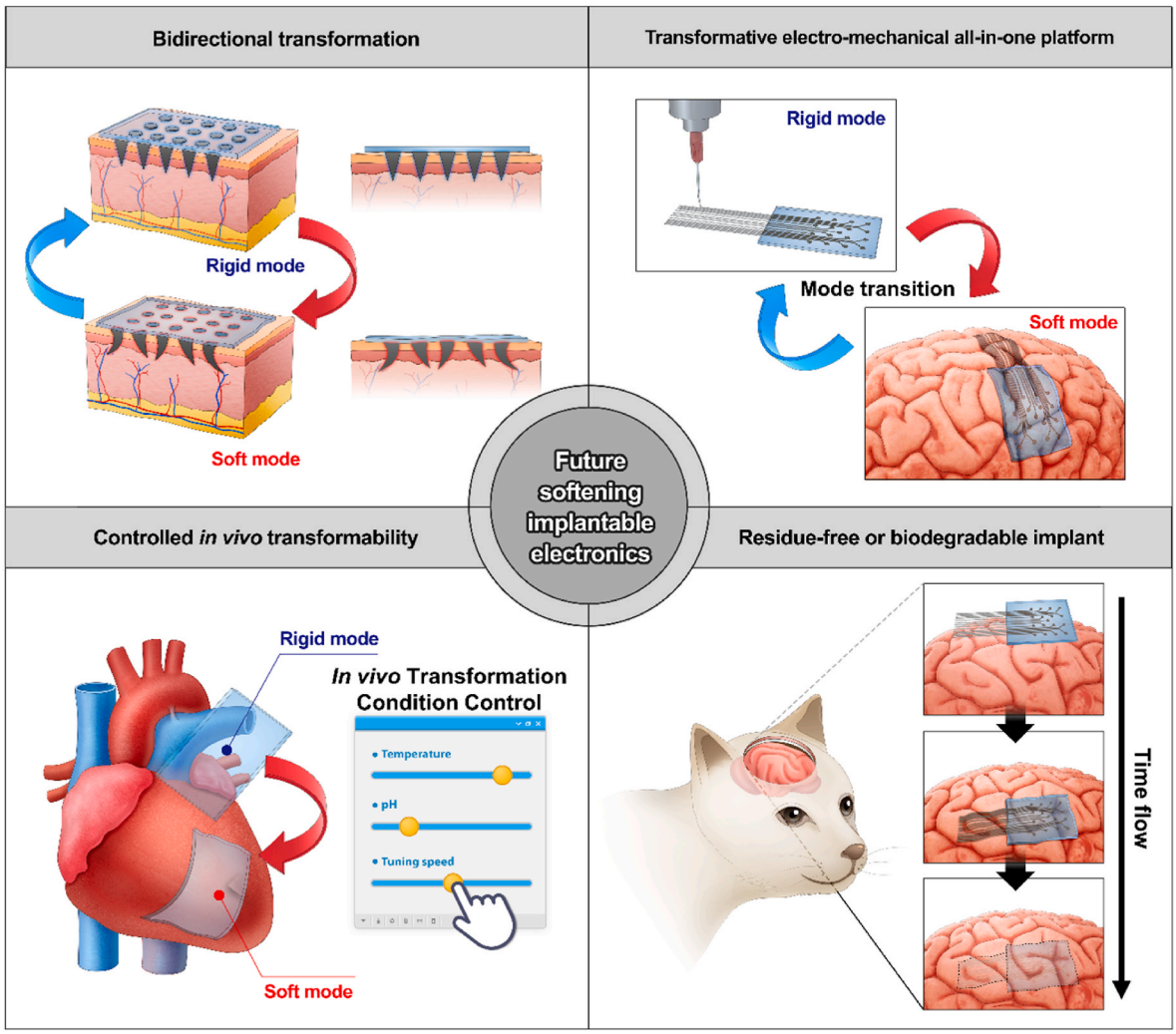

Fig. 6. Future development directions for the next-generation softening implantable bioelectronics. Four essential features for future advancements include bidirectional mechanical tunability, all-in-one electro-mechanical functionality, controlled *in vivo* transformability, and residue-free integration or biodegradability.

Bidirectional transformation of bioelectronics is pivotal for achieving reusable softening bioelectronics. Current softening devices, such as those with dissolvable stiffeners (Shi et al., 2019; Cointe et al., 2022), often undergo a one-time transition from rigid to soft, limiting them to a single use. Integrating bidirectional transformable materials holds the potential for multiple uses through stimuli-responsive adjustments between rigid and soft states. Furthermore, in tackling the design and fabrication inefficiency observed in most of softening bioelectronics, where separate electrical circuits and mechanical frameworks are assembled together (Byun et al., 2019), it becomes crucial to incorporate a transformative electro-mechanical all-in-one platform. Recent efforts, such as the exploration of liquid metal gallium as a potential candidate for such platforms (Kwon et al., 2024), signify the beginning of this transformative approach. However, extensive research into a variety of dual-functional materials is necessary to establish a robust foundation for the creation of compact, reusable, and transformative bioelectronic devices.

Moreover, the future development of softening implantable electronics requires biological safe and in-body-compatible triggering mechanism, with controlled *in vivo* transformability being a crucial feature. Existing studies often employ stimuli conditions that do not align with human physiological conditions, requiring high temperatures above 40 °C for softening (Reeder et al., 2014) or light-responsive materials unfit for internal body use (Ruan et al., 2019). Additionally, water-responsive materials present challenges for precision-targeted applications, as they soften spontaneously upon entering the body. Ensuring safe and controlled softening within the body's environment is essential to improve the safety and efficacy of bioelectronics in practical applications. Furthermore, using residue-free or biodegradable material is key for safe in-body applications. Devices designed with fully biodegradable or excretable materials increase biocompatibility by eliminating the need for secondary surgery for device removal (Yang et al., 2022). This is particularly suitable for short-term applications like temporary medical implants, such as biodegradable stents (Zong et al., 2022), bioresorbable pressure sensors (Shin et al., 2019), and many others.

Surmounting these challenges is pivotal, not only for enhancing the functionality and adaptability of softening bioelectronics, but also for ensuring their safety and compatibility for human use. Moving forward, existing wireless power transmission systems can be potentially exploited to enhance the long-term in-body operation of softening implantable systems (Qazi et al., 2022; Kim et al., 2021). Furthermore, wireless data communication technology including Bluetooth and radiofrequency identification can enable periodic transmission of physiological signals to monitor the health condition of patients (Yoo et al., 2021; Lu et al., 2021). These advancements facilitate the evolution of bioelectronics beyond implantable devices to next-generation bioelectronics that integrate seamlessly with the body, offering highly sophisticated physical and functional interfaces with biological tissues for desired purposes. This evolution in softening bioelectronics is poised to

revolutionize the biomedical devices, providing more advanced and efficient solutions in medical technology. Ultimately, this will enhance patient care and propel the field of medical technology forward. While our discussion has primarily focused on implantable bioelectronics, the transformative nature of softening technology holds significant promise for various applications beyond this realm, particularly in soft robotics (Shen et al., 2020), sensors (Hu et al., 2019; Toma et al., 2013), actuators (Hu et al., 2019; Jiang et al., 2016), and artificial muscles (Islam et al., 2013), potentially leading to innovations that enhance the adaptability and functionality of devices across the fields.

CRediT authorship contribution statement

Subin Oh: Writing – review & editing, Writing – original draft, Visualization, Project administration, Investigation, Conceptualization. **Simok Lee:** Writing – review & editing, Writing – original draft, Visualization, Investigation, Conceptualization. **Sung Woo Kim:** Visualization, Investigation. **Choong Yeon Kim:** Writing – review & editing, Investigation. **Eun Young Jeong:** Visualization, Investigation. **Juhyun Lee:** Investigation. **Do A Kwon:** Writing – review & editing. **Jae-Woong Jeong:** Writing – review & editing, Visualization, Supervision, Project administration, Investigation, Funding acquisition, Conceptualization.

Declaration of competing interest

The authors declare that they have no known competing financial interests or personal relationships that could have appeared to influence the work reported in this paper.

Data availability

The authors do not have permission to share data.

Acknowledgements

This work was supported by National Research Foundation of Korea (NRF-2022M3E5E9017759 and NRF–2022R1A4A5033852), Institute of Information and Communications Technology Planning and Evaluation (IITP-2022-0-00025), and an internal grant of Electronics and Telecommunications Research Institute (22RB1100, Exploratory and Strategic Research of ETRI-KAIST ICT Future Technology).

References

Acharya, S., Roberts, P., Rane, T., Singhal, R., Hong, P., Ranade, V., Majidi, C., Webster-Wood, V., Reeja-Jayan, B., 2023. Gecko adhesion-based sea star crawler robot. Front. Robot. AI 10.

Agno, K.-C., Yang, K., Byun, S.-H., Oh, S., Lee, S., Kim, H., Kim, K., Cho, S., Jeong, W.-I., Jeong, J.-W., 2023. A temperature-responsive intravenous needle that irreversibly softens on insertion. Nat. Biomed. Eng. 1–14. https://doi.org/10.1038/s41551-023-01116-z.

Ahn, Y., Jang, Y., Selvapalam, N., Yun, G., Kim, K., 2013. Supramolecular Velcro for reversible underwater adhesion. Angew. Chem., Int. Ed. 52, 3140–3144. https://doi.org/10.1002/anie.201209382.

Arai, T., Freddi, G., Innocenti, R., Tsukada, M., 2004. Biodegradation of Bombyx mori silk fibroin fibers and films. J. Appl. Polym. Sci. 91, 2383–2390. https://doi.org/10.1002/app.13393.

Archer, E., Torretti, M., Madbouly, S., 2023. Biodegradable polycaprolactone (PCL) based polymer and composites. Phys. Sci. Rev. 8, 4391–4414. https://doi.org/10.1515/psr-2020-0074.

Asakura, T., Endo, M., Tasei, Y., Ohkubo, T., Hiraoki, T., 2017. Hydration of Bombyx mori silk cocoon, silk sericin and silk fibroin and their interactions with water as studied by 13C NMR and 2H NMR relaxation. J. Mater. Chem. B 5, 1624–1632. https://doi.org/10.1039/C6TB03266D.

Butylina, S., Geng, S., Oksman, K., 2016. Properties of as-prepared and freeze-dried hydrogels made from poly(vinyl alcohol) and cellulose nanocrystals using freeze-thaw technique. Eur. Polym. J. 81, 386–396. https://doi.org/10.1016/j.eurpolymj.2016.06.028.

Byun, S.-H., Sim, J.Y., Zhou, Z., Lee, J., Qazi, R., Walicki, M.C., Parker, K.E., Haney, M.P., Choi, S.H., Shon, A., Gereau, G.B., Bilbily, J., Li, S., Liu, Y., Yeo, W.-H., McCall, J.G., Xiao, J., Jeong, J.-W., 2019. Mechanically transformative electronics, sensors, and implantable devices. Sci. Adv. 5, eaay0418 https://doi.org/10.1126/sciadv.aay0418.

Byun, S.-H., Sim, J.Y., Agno, K.-C., Jeong, J.-W., 2020. Materials and manufacturing strategies for mechanically transformative electronics. Mater. Today Adv. 7, 100089 https://doi.org/10.1016/j.mtadv.2020.100089.

Byun, S.-H., Kim, C.S., Agno, K.-C., Lee, S., Li, Z., Cho, B.J., Jeong, J.-W., 2021. Design strategy for transformative electronic system toward rapid, bidirectional stiffness tuning using graphene and flexible thermoelectric device interfaces. Adv. Mater. 33, 2007239 https://doi.org/10.1002/adma.202007239.

Cao, Y., Wang, B., 2009. Biodegradation of silk biomaterials. Int. J. Mol. Sci. 10, 1514–1524. https://doi.org/10.3390/ijms10041514.

Carlyon, R.P., Goehring, T., 2021. Cochlear implant research and development in the twenty-first century: a critical update. JARO 22, 481–508. https://doi.org/10.1007/s10162-021-00811-5.

Chen, Y.-C., Yang, H., 2017. Octopus-inspired assembly of nanosucker arrays for dry/wet adhesion. ACS Nano 11, 5332–5338. https://doi.org/10.1021/acsnano.7b00809.

Chen, X., Hu, S., Li, L., Torkelson, J.M., 2020. Dynamic covalent polyurethane networks with excellent property and cross-link density recovery after recycling and potential for monomer recovery. ACS Appl. Polym. Mater. 2, 2093–2101. https://doi.org/10.1021/acsapm.0c00378.

Chen, S., Zhao, R., Sun, X., Wang, H., Li, L., Liu, J., 2023. Toxicity and biocompatibility of liquid metals. Adv. Healthcare Mater. 12, 2201924 https://doi.org/10.1002/adhm.202201924.

Choi, S., Kim, B., Park, S., Seo, J.-H., Ahn, S., 2022. Slidable cross-linking effect on liquid crystal elastomers: enhancement of toughness, shape-memory, and self-healing properties. ACS Appl. Mater. Interfaces 14, 32486–32496. https://doi.org/10.1021/acsami.2c06462.

Choi, H., Kim, Y., Kim, S., Jung, H., Lee, S., Kim, K., Han, H.-S., Kim, J.Y., Shin, M., Son, D., 2023. Adhesive bioelectronics for sutureless epicardial interfacing. Nat. Electron. 6, 779–789. https://doi.org/10.1038/s41928-023-01023-w.

Chung, W.G., Kim, E., Kwon, Y.W., Lee, J., Lee, S., Jeong, I., Park, J.-U., 2023. Ga-based liquid metals: versatile and biocompatible solutions for next-generation bioelectronics. Adv. Funct. Mater. n/a, 307990. https://doi.org/10.1002/adfm.202307990.

Cianchetti, M., Ranzani, T., Gerboni, G., De Falco, I., Laschi, C., Menciassi, A., 2013. STIFF-FLOP surgical manipulator: mechanical design and experimental characterization of the single module. In: 2013 IEEE/RSJ International Conference on Intelligent Robots and Systems. Presented at the 2013 IEEE/RSJ International Conference on Intelligent Robots and Systems, pp. 3576–3581. https://doi.org/10.1109/IROS.2013.6696866.

Cointe, C., Laborde, A., Nowak, L.G., Arvanitis, D.N., Bourrier, D., Bergaud, C., Maziz, A., 2022. Scalable batch fabrication of ultrathin flexible neural probes using a bioresorbable silk layer. Microsyst. Nanoeng. 8, 1–11. https://doi.org/10.1038/s41378-022-00353-7.

Dagnon, K.L., Shanmuganathan, K., Weder, C., Rowan, S.J., 2012. Water-triggered modulus changes of cellulose nanofiber nanocomposites with hydrophobic polymer matrices. Macromolecules 45, 4707–4715. https://doi.org/10.1021/ma300463y.

Deng, J., Yuk, H., Wu, J., Varela, C.E., Chen, X., Roche, E.T., Guo, C.F., Zhao, X., 2021. Electrical bioadhesive interface for bioelectronics. Nat. Mater. 20, 229–236. https://doi.org/10.1038/s41563-020-00814-2.

Deng, H., Huang, K., Xiu, L., Sun, W., Yao, Q., Fang, X., Huang, X., Noreldeen, H.A.A., Peng, H., Xie, J., Chen, W., 2022a. Bis-Schiff base linkage-triggered highly bright luminescence of gold nanoclusters in aqueous solution at the single-cluster level. Nat. Commun. 13, 3381. https://doi.org/10.1038/s41467-022-30760-3.

Deng, J., Zhu, E.-Q., Xu, G.-F., Naik, N., Murugadoss, V., Ma, M.-G., Guo, Z., Shi, Z.-J., 2022b. Overview of renewable polysaccharide-based composites for biodegradable food packaging applications. Green Chem. 24, 480–492. https://doi.org/10.1039/D1GC03898B.

Do, D.-H., Ecker, M., Voit, W.E., 2017. Characterization of a thiol-ene/acrylate-based polymer for neuroprosthetic implants. ACS Omega 2, 4604–4611. https://doi.org/10.1021/acsomega.7b00834.

Doucet, L., Carlotti, G., 1994. Elastic properties of silicate glass and spin-on glass thin films. MRS Online Proc. Libr. 356, 215–220. https://doi.org/10.1557/PROC-356-215.

Elsner, N., Kozlovskaya, V., A. Sukhishvili, S., Fery, A., 2006. pH-Triggered softening of crosslinked hydrogen-bonded capsules. Soft Matter 2, 966–972. https://doi.org/10.1039/B608317J.

Gaeta L. J, T., McDonald, K., Kinnicutt, L., Le, M., Wilkinson-Flicker, S., Jiang, Y., Atakuru, T., Samur, E., Ranzani, T., 2023. Magnetically induced stiffening for soft robotics. Soft Matter 19, 2623–2636. https://doi.org/10.1039/D2SM01390H.

Gao, M., Wu, H., Plamthottam, R., Xie, Z., Liu, Y., Hu, J., Wu, S., Wu, L., He, X., Pei, Q., 2021. Skin temperature-triggered, debonding-on-demand sticker for a self-powered mechanosensitive communication system. Matter 4, 1962–1974. https://doi.org/10.1016/j.matt.2021.03.003.

Gao, M., Meng, Y., Shen, C., Pei, Q., 2022. Stiffness variable polymers comprising phase-changing side-chains: material syntheses and application explorations. Adv. Mater. 34, 2109798 https://doi.org/10.1002/adma.202109798.

Garcia-Sandoval, A., Pal, A., Mishra, A.M., Sherman, S., Parikh, A.R., Joshi-Imre, A., Arreaga-Salas, D., Gutierrez-Heredia, G., Duran-Martinez, A.C., Nathan, J., Hosseini, S.M., Carmel, J.B., Voit, W., 2018. Chronic softening spinal cord stimulation arrays. J. Neural. Eng. 15, 045002 https://doi.org/10.1088/1741-2552/aab90d.

Garcia-Sandoval, A., Guerrero, E., Hosseini, S.M., Rocha-Flores, P.E., Rihani, R., Black, B. J., Pal, A., Carmel, J.B., Pancrazio, J.J., Voit, W.E., 2021. Stable softening bioelectronics: a paradigm for chronically viable ester-free neural interfaces such as

spinal cord stimulation implants. Biomaterials 277, 121073. https://doi.org/10.1016/j.biomaterials.2021.121073.
González-González, M.A., Kanneganti, A., Joshi-Imre, A., Hernandez-Reynoso, A.G., Bendale, G., Modi, R., Ecker, M., Khurram, A., Cogan, S.F., Voit, W.E., Romero-Ortega, M.I., 2018. Thin film multi-electrode softening cuffs for selective neuromodulation. Sci. Rep. 8, 16390 https://doi.org/10.1038/s41598-018-34566-6.
Guo, Z., Wang, F., Wang, L., Tu, K., Jiang, C., Xi, Y., Hong, W., Xu, Q., Wang, X., Yang, B., Sun, B., Lin, Z., Liu, J., 2022. A flexible neural implant with ultrathin substrate for low-invasive brain–computer interface applications. Microsyst. Nanoeng. 8, 1–12. https://doi.org/10.1038/s41378-022-00464-1.
Han, X.-J., Dong, Z.-Q., Fan, M.-M., Liu, Y., Li, J.-H., Wang, Y.-F., Yuan, Q.-J., Li, B.-J., Zhang, S., 2012. pH-induced shape-memory polymers. Macromol. Rapid Commun. 33, 1055–1060. https://doi.org/10.1002/marc.201200153.
Harris, J.P., Hess, A.E., Rowan, S.J., Weder, C., Zorman, C.A., Tyler, D.J., Capadona, J.R., 2011. In vivo deployment of mechanically adaptive nanocomposites for intracortical microelectrodes. J. Neural. Eng. 8, 046010 https://doi.org/10.1088/1741-2560/8/4/046010.
Herbert, K.M., Fowler, H.E., McCracken, J.M., Schlafmann, K.R., Koch, J.A., White, T.J., 2022a. Synthesis and alignment of liquid crystalline elastomers. Nat. Rev. Mater. 7, 23–38. https://doi.org/10.1038/s41578-021-00359-z.
Herbert, R., Lim, H.-R., Rigo, B., Yeo, W.-H., 2022b. Fully implantable wireless batteryless vascular electronics with printed soft sensors for multiplex sensing of hemodynamics. Sci. Adv. 8, eabm1175 https://doi.org/10.1126/sciadv.abm1175.
Hess, A.E., Capadona, J.R., Shanmuganathan, K., Hsu, L., Rowan, S.J., Weder, C., Tyler, D.J., Zorman, C.A., 2011. Development of a stimuli-responsive polymer nanocomposite toward biologically optimized, MEMS-based neural probes. J. Micromech. Microeng. 21, 054009 https://doi.org/10.1088/0960-1317/21/5/054009.
Hess-Dunning, A., Tyler, D.J., 2018. A mechanically-adaptive polymer nanocomposite-based intracortical probe and package for chronic neural recording. Micromachines 9, 583. https://doi.org/10.3390/mi9110583.
Hosseini, E.S., Dervin, S., Ganguly, P., Dahiya, R., 2021. Biodegradable materials for sustainable health monitoring devices. ACS Appl. Bio Mater. 4, 163–194. https://doi.org/10.1021/acsabm.0c01139.
Hu, W., Ren, Z., Li, J., Askounis, E., Xie, Z., Pei, Q., 2015. New dielectric elastomers with variable moduli. Adv. Funct. Mater. 25, 4827–4836. https://doi.org/10.1002/adfm.201501530.
Hu, X., Zhou, J., Vatankhah-Varnosfaderani, M., Daniel, W.F.M., Li, Q., Zhushma, A.P., Dobrynin, A.V., Sheiko, S.S., 2016. Programming temporal shapeshifting. Nat. Commun. 7, 12919 https://doi.org/10.1038/ncomms12919.
Hu, L., Zhang, Q., Li, X., Serpe, M.J., 2019. Stimuli-responsive polymers for sensing and actuation. Mater. Horiz. 6, 1774–1793. https://doi.org/10.1039/C9MH00490D.
Hwang, S.-W., Kang, S.-K., Huang, X., Brenckle, M.A., Omenetto, F.G., Rogers, JohnA., 2015. Materials for programmed, functional transformation in transient electronic systems. Adv. Mater. 27, 47–52. https://doi.org/10.1002/adma.201403051.
Hwang, D., Barron, E.J., Haque, A.B.M.T., Bartlett, M.D., 2022. Shape morphing mechanical metamaterials through reversible plasticity. Sci. Robot. 7, eabg2171 https://doi.org/10.1126/scirobotics.abg2171.
Islam, M.R., Li, X., Smyth, K., Serpe, M.J., 2013. Polymer-based muscle expansion and contraction. Angew. Chem. Int. Ed. 52, 10330–10333. https://doi.org/10.1002/anie.201303475.
Jayasri, D., Satyavathi, N., Sastry, V.S.S., Murthy, K.P.N., 2009. Phase transition in liquid crystal elastomers—a Monte Carlo study employing non-Boltzmann sampling. Phys. Stat. Mech. Appl. 388, 385–391. https://doi.org/10.1016/j.physa.2008.10.039.
Jeong, J.-W., McCall, J.G., Shin, G., Zhang, Y., Al-Hasani, R., Kim, M., Li, S., Sim, J.Y., Jang, K.-I., Shi, Y., Hong, D.Y., Liu, Y., Schmitz, G.P., Xia, L., He, Z., Gamble, P., Ray, W.Z., Huang, Y., Bruchas, M.R., Rogers, J.A., 2015. Wireless optofluidic systems for programmable in vivo pharmacology and optogenetics. Cell 162, 662–674. https://doi.org/10.1016/j.cell.2015.06.058.
Jiang, Y., Hu, C., Cheng, H., Li, C., Xu, T., Zhao, Y., Shao, H., Qu, L., 2016. Spontaneous, straightforward fabrication of partially reduced graphene oxide–polypyrrole composite films for versatile actuators. ACS Nano 10, 4735–4741. https://doi.org/10.1021/acsnano.6b01233.
Jiao, Y., Zhang, Y., Feng, H., Li, H., Wang, Z., Wang, P., Wang, Y., Zheng, N., Xie, T., Ma, Y., Feng, X., 2023. A multifunctional bioelectronic device with switchable rigidity and reconfigurable shapes for comprehensive diagnosis. Adv. Electron. Mater. 9, 2201343 https://doi.org/10.1002/aelm.202201343.
Joo, H., Lee, Y., Kim, J., Yoo, J.-S., Yoo, S., Kim, Sangyeon, Arya, A.K., Kim, Sangjun, Choi, S.H., Lu, N., Lee, H.S., Kim, Sanghoek, Lee, S.-T., Kim, D.-H., 2021. Soft implantable drug delivery device integrated wirelessly with wearable devices to treat fatal seizures. Sci. Adv. 7, eabd4639 https://doi.org/10.1126/sciadv.abd4639.
Kang, S.-K., Hwang, S.-W., Yu, S., Seo, J.-H., Corbin, E.A., Shin, J., Wie, D.S., Bashir, R., Ma, Z., Rogers, J.A., 2015. Biodegradable thin metal foils and spin-on glass materials for transient electronics. Adv. Funct. Mater. 25, 1789–1797. https://doi.org/10.1002/adfm.201403469.
Keridou, I., Franco, L., del Valle, L.J., Martínez, J.C., Funk, L., Turon, P., Puiggalí, J., 2020. Microstructural changes during degradation of biobased poly(4-hydroxybutyrate) sutures. Polymers 12, 2024. https://doi.org/10.3390/polym12092024.
Kim, Y., Zhao, X., 2022. Magnetic soft materials and robots. Chem. Rev. 122, 5317–5364. https://doi.org/10.1021/acs.chemrev.1c00481.
Kim, D.-H., Viventi, J., Amsden, J.J., Xiao, J., Vigeland, L., Kim, Y.-S., Blanco, J.A., Panilaitis, B., Frechette, E.S., Contreras, D., Kaplan, D.L., Omenetto, F.G., Huang, Y., Hwang, K.-C., Zakin, M.R., Litt, B., Rogers, J.A., 2010. Dissolvable films of silk fibroin for ultrathin conformal bio-integrated electronics. Nat. Mater. 9, 511–517. https://doi.org/10.1038/nmat2745.
Kim, M., Doh, J., Lee, D., 2016. pH-induced softening of polyelectrolyte microcapsules without apparent swelling. ACS Macro Lett. 5, 487–492. https://doi.org/10.1021/acsmacrolett.6b00124.
Kim, H., Lee, H.S., Jeon, Y., Park, W., Zhang, Y., Kim, B., Jang, H., Xu, B., Yeo, Y., Kim, D. R., Lee, C.H., 2020. Bioresorbable, miniaturized porous silicon needles on a flexible water-soluble backing for unobtrusive, sustained delivery of chemotherapy. ACS Nano 14, 7227–7236. https://doi.org/10.1021/acsnano.0c02343.
Kim, C.Y., Ku, M.J., Qazi, R., Nam, H.J., Park, J.W., Nam, K.S., Oh, S., Kang, I., Jang, J.-H., Kim, W.Y., Kim, J.-H., Jeong, J.-W., 2021. Soft subdermal implant capable of wireless battery charging and programmable controls for applications in optogenetics. Nat. Commun. 12, 535. https://doi.org/10.1038/s41467-020-20803-y.
Kim, I.H., Choi, S., Lee, J., Jung, J., Yeo, J., Kim, J.T., Ryu, S., Ahn, S., Kang, J., Poulin, P., Kim, S.O., 2022. Human-muscle-inspired single fibre actuator with reversible percolation. Nat. Nanotechnol. 17, 1198–1205. https://doi.org/10.1038/s41565-022-01220-2.
Kim, Kiho, Min, I.S., Kim, T.H., Kim, D.H., Hwang, S., Kang, K., Kim, Kyubeen, Park, S., Lee, J., Cho, Y.U., Lee, J.W., Yeo, W.-H., Song, Y.M., Jung, Y., Yu, K.J., 2023. Fully implantable and battery-free wireless optoelectronic system for modulable cancer therapy and real-time monitoring. npj Flex. Electron. 7, 1–12. https://doi.org/10.1038/s41528-023-00276-x.
Kotikian, A., Truby, R.L., Boley, J.W., White, T.J., Lewis, J.A., 2018. 3D printing of liquid crystal elastomeric actuators with spatially programed nematic order. Adv. Mater. 30, 1706164 https://doi.org/10.1002/adma.201706164.
Kuang, X., Wu, S., Ze, Q., Yue, L., Jin, Y., Montgomery, S.M., Yang, F., Qi, H.J., Zhao, R., 2021. Magnetic dynamic polymers for modular assembling and reconfigurable morphing architectures. Adv. Mater. 33, 2102113 https://doi.org/10.1002/adma.202102113.
Kwon, D.A., Lee, S., Kim, C.Y., Kang, I., Park, S., Jeong, J.-W., 2024. Body-temperature softening electronic ink for additive manufacturing of transformative bioelectronics via direct writing. Sci. Adv. 10, eadn1186 https://doi.org/10.1126/sciadv.adn1186.
Lai, J.-C., Li, L., Wang, D.-P., Zhang, M.-H., Mo, S.-R., Wang, X., Zeng, K.-Y., Li, C.-H., Jiang, Q., You, X.-Z., Zuo, J.-L., 2018. A rigid and healable polymer cross-linked by weak but abundant Zn(II)-carboxylate interactions. Nat. Commun. 9, 2725. https://doi.org/10.1038/s41467-018-05285-3.
Lee, K.Y., Rowley, J.A., Eiselt, P., Moy, E.M., Bouhadir, K.H., Mooney, D.J., 2000. Controlling mechanical and swelling properties of alginate hydrogels independently by cross-linker type and cross-linking density. Macromolecules 33, 4291–4294. https://doi.org/10.1021/ma9921347.
Lee, J., Parker, K.E., Kawakami, C., Kim, J.R., Qazi, R., Yea, J., Zhang, S., Kim, C.Y., Bilbily, J., Xiao, J., Jang, K.-I., McCall, J.G., Jeong, J.-W., 2020. Rapidly customizable, scalable 3D-printed wireless optogenetic probes for versatile applications in neuroscience. Adv. Funct. Mater. 30, 2004285 https://doi.org/10.1002/adfm.202004285.
Lee, Y., Kang, T., Cho, H.R., Lee, G.J., Park, O.K., Kim, S., Lee, B., Kim, H.M., Cha, G.D., Shin, Y., Lee, W., Kim, M., Kim, H., Song, Y.M., Choi, S.H., Hyeon, T., Kim, D.-H., 2021. Localized delivery of theranostic nanoparticles and high-energy photons using microneedles-on-bioelectronics. Adv. Mater. 33, 2100425 https://doi.org/10.1002/adma.202100425.
Lee, S., Byun, S.-H., Kim, C.Y., Cho, S., Park, S., Sim, J.Y., Jeong, J.-W., 2022a. Beyond human touch perception: an adaptive robotic skin based on gallium microgranules for pressure sensory augmentation. Adv. Mater. 34, 2204805 https://doi.org/10.1002/adma.202204805.
Lee, W., Kim, H., Kang, I., Park, Hongjun, Jung, J., Lee, H., Park, Hyunchang, Park, J.S., Yuk, J.M., Ryu, S., Jeong, J.-W., Kang, J., 2022b. Universal assembly of liquid metal particles in polymers enables elastic printed circuit board. Science 378, 637–641. https://doi.org/10.1126/science.abo6631.
Li, S., Bai, H., Liu, Z., Zhang, X., Huang, C., Wiesner, L.W., Silberstein, M., Shepherd, R. F., 2021a. Digital light processing of liquid crystal elastomers for self-sensing artificial muscles. Sci. Adv. 7, eabg3677 https://doi.org/10.1126/sciadv.abg3677.
Li, Y., Li, N., De Oliveira, N., Wang, S., 2021b. Implantable bioelectronics toward long-term stability and sustainability. Matter 4, 1125–1141. https://doi.org/10.1016/j.matt.2021.02.001.
Lima, D.S., Tenório-Neto, E.T., Lima-Tenório, M.K., Guilherme, M.R., Scariot, D.B., Nakamura, C.V., Muniz, E.C., Rubira, A.F., 2018. pH-responsive alginate-based hydrogels for protein delivery. J. Mol. Liq. 262, 29–36. https://doi.org/10.1016/j.molliq.2018.04.002.
Liu, H., Tian, H., Li, X., Chen, X., Zhang, K., Shi, H., Wang, C., Shao, J., 2022a. Shape-programmable, deformation-locking, and self-sensing artificial muscle based on liquid crystal elastomer and low–melting point alloy. Sci. Adv. 8, eabn5722 https://doi.org/10.1126/sciadv.abn5722.
Liu, Y., Chen, T., Jin, Z., Li, M., Zhang, D., Duan, L., Zhao, Z., Wang, C., 2022b. Tough, stable and self-healing luminescent perovskite-polymer matrix applicable to all harsh aquatic environments. Nat. Commun. 13, 1338. https://doi.org/10.1038/s41467-022-29084-z.
Lu, W., Bai, W., Zhang, H., Xu, C., Chiarelli, A.M., Vázquez-Guardado, A., Xie, Z., Shen, H., Nandoliya, K., Zhao, H., Lee, K., Wu, Y., Franklin, D., Avila, R., Xu, S., Rwei, A., Han, M., Kwon, K., Deng, Y., Yu, X., Thorp, E.B., Feng, X., Huang, Y., Forbess, J., Ge, Z.-D., Rogers, J.A., 2021. Wireless, implantable catheter-type oximeter designed for cardiac oxygen saturation. Sci. Adv. 7, eabe0579 https://doi.org/10.1126/sciadv.abe0579.
Luckachan, G.E., Pillai, C.K.S., 2011. Biodegradable polymers- A review on recent trends and emerging perspectives. J. Polym. Environ. 19, 637–676. https://doi.org/10.1007/s10924-011-0317-1.
Mattmann, M., De Marco, C., Briatico, F., Tagliabue, S., Colusso, A., Chen, X.-Z., Lussi, J., Chautems, C., Pané, S., Nelson, B., 2022. Thermoset shape memory polymer variable

stiffness 4D robotic catheters. Adv. Sci. 9, 2103277 https://doi.org/10.1002/advs.202103277.
Mistry, D., Traugutt, N.A., Sanborn, B., Volpe, R.H., Chatham, L.S., Zhou, R., Song, B., Yu, K., Long, K.N., Yakacki, C.M., 2021. Soft elasticity optimises dissipation in 3D-printed liquid crystal elastomers. Nat. Commun. 12, 6677. https://doi.org/10.1038/s41467-021-27013-0.
Nakajima, M., Usami, M., Nakazawa, K., Arishima, K., Yamamoto, M., 2008. Developmental toxicity of indium: embryotoxicity and teratogenicity in experimental animals. Congenital. Anom. 48, 145–150. https://doi.org/10.1111/j.1741-4520.2008.00197.x.
Nguyen, J.K., Park, D.J., Skousen, J.L., Hess-Dunning, A.E., Tyler, D.J., Rowan, S.J., Weder, C., Capadona, J.R., 2014. Mechanically-compliant intracortical implants reduce the neuroinflammatory response. J. Neural. Eng. 11, 056014 https://doi.org/10.1088/1741-2560/11/5/056014.
Nisar, S., Pandit, Ashiq Hussain, Nadeem, M., Pandit, Altaf Hussain, Rizvi, M.M.A., Rattan, S., 2021. γ-Radiation induced L-glutamic acid grafted highly porous, pH-responsive chitosan hydrogel beads: a smart and biocompatible vehicle for controlled anti-cancer drug delivery. Int. J. Biol. Macromol. 182, 37–50. https://doi.org/10.1016/j.ijbiomac.2021.03.134.
Nishiguchi, A., Ichimaru, H., Ito, S., Nagasaka, K., Taguchi, T., 2022. Hotmelt tissue adhesive with supramolecularly-controlled sol-gel transition for preventing postoperative abdominal adhesion. Acta Biomater. 146, 80–93. https://doi.org/10.1016/j.actbio.2022.04.037.
Nurlidar, F., Rahayu, D.P., Lasmawati, D., Yunus, A.L., Heryani, R., Suryani, N., 2023. A simple method for the simultaneous encapsulation of ciprofloxacin into PEGDA/alginate hydrogels using gamma irradiation. Arab. J. Chem. 16, 104793 https://doi.org/10.1016/j.arabjc.2023.104793.
Oh, S., Lee, Sunwoo, Byun, S.-H., Lee, Simok, Kim, C.Y., Yea, J., Chung, S., Li, S., Jang, K.-I., Kang, J., Jeong, J.-W., 2023. 3D shape-morphing display enabled by electrothermally responsive, stiffness-tunable liquid metal platform with stretchable electroluminescent device. Adv. Funct. Mater. 33, 2214766 https://doi.org/10.1002/adfm.202214766.
Opdahl, A., Kim, S.H., Koffas, T.S., Marmo, C., Somorjai, G.A., 2003. Surface mechanical properties of pHEMA contact lenses: viscoelastic and adhesive property changes on exposure to controlled humidity. J. Biomed. Mater. Res., Part A 67A, 350–356. https://doi.org/10.1002/jbm.a.10054.
Pang, C., Koo, J.H., Nguyen, A., Caves, J.M., Kim, M.-G., Chortos, A., Kim, K., Wang, P.J., Tok, J.B.-H., Bao, Z., 2015. Highly skin-conformal microhairy sensor for pulse signal amplification. Adv. Mater. 27, 634–640. https://doi.org/10.1002/adma.201403807.
Park, S., Yuk, H., Zhao, R., Yim, Y.S., Woldeghebriel, E.W., Kang, J., Canales, A., Fink, Y., Choi, G.B., Zhao, X., Anikeeva, P., 2021. Adaptive and multifunctional hydrogel hybrid probes for long-term sensing and modulation of neural activity. Nat. Commun. 12, 3435. https://doi.org/10.1038/s41467-021-23802-9.
Park, S.J., Im, S.H., Kim, D., Park, D., Jung, Y., Han, H., Kim, S.H., Chung, J.J., 2023. Tough and biodegradable polyurethane-silica hybrids with a rapid sol-gel transition for bone repair. NPG Asia Mater. 15, 1–19. https://doi.org/10.1038/s41427-023-00475-y.
Qazi, R., Parker, K.E., Kim, C.Y., Rill, R., Norris, M.R., Chung, J., Bilbily, J., Kim, J.R., Walicki, M.C., Gereau, G.B., Lim, H., Xiong, Y., Lee, J.R., Tapia, M.A., Kravitz, A.V., Will, M.J., Ha, S., McCall, J.G., Jeong, J.-W., 2022. Scalable and modular wireless-network infrastructure for large-scale behavioural neuroscience. Nat. Biomed. Eng. 6, 771–786. https://doi.org/10.1038/s41551-021-00814-w.
Qiu, Y., Askounis, E., Guan, F., Peng, Z., Xiao, W., Pei, Q., 2020. Dual-stimuli-responsive polymer composite with ultrawide tunable stiffness range triggered by water and temperature. ACS Appl. Polym. Mater. 2, 2008–2015. https://doi.org/10.1021/acsapm.0c00181.
Reeder, J., Kaltenbrunner, M., Ware, T., Arreaga-Salas, D., Avendano-Bolivar, A., Yokota, T., Inoue, Y., Sekino, M., Voit, W., Sekitani, T., Someya, T., 2014. Mechanically adaptive organic transistors for implantable electronics. Adv. Mater. 26, 4967–4973. https://doi.org/10.1002/adma.201400420.
Reit, R., Abitz, H., Reddy, N., Parker, S., Wei, A., Aragon, N., Ho, M., Weittenhiller, A., Kang, T., Ecker, M., Voit, W.E., 2016. Thiol–epoxy/maleimide ternary networks as softening substrates for flexible electronics. J. Mater. Chem. B 4, 5367–5374. https://doi.org/10.1039/C6TB01082B.
Ren, Z., Hu, W., Liu, C., Li, S., Niu, X., Pei, Q., 2016. Phase-changing bistable electroactive polymer exhibiting sharp rigid-to-rubbery transition. Macromolecules 49, 134–140. https://doi.org/10.1021/acs.macromol.5b02382.
Riley, L., Schirmer, L., Segura, T., 2019. Granular hydrogels: emergent properties of jammed hydrogel microparticles and their applications in tissue repair and regeneration. Curr. Opin. Biotechnol., Pharmaceutical Biotechnology ● Chemical Biotechnology 60, 1–8. https://doi.org/10.1016/j.copbio.2018.11.001.
Rohr, O., 2002. Bismuth – the new ecologically green metal for modern lubricating engineering. Ind. Lubric. Tribol. 54, 153–164. https://doi.org/10.1108/00368790210431709.
Rotundo, S., Brizi, D., Flori, A., Giovannetti, G., Menichetti, L., Monorchio, A., 2022. Shaping and focusing magnetic field in the human body: state-of-the art and promising technologies. Sensors 22, 5132. https://doi.org/10.3390/s22145132.
Ruan, C., Liu, C., Hu, H., Guo, X.-L., Jiang, B.-P., Liang, H., Shen, X.-C., 2019. NIR-II light-modulated thermosensitive hydrogel for light-triggered cisplatin release and repeatable chemo-photothermal therapy. Chem. Sci. 10, 4699–4706. https://doi.org/10.1039/C9SC00375D.
Ryu, H., Park, H., Kim, M.-K., Kim, B., Myoung, H.S., Kim, T.Y., Yoon, H.-J., Kwak, S.S., Kim, J., Hwang, T.H., Choi, E.-K., Kim, S.-W., 2021. Self-rechargeable cardiac pacemaker system with triboelectric nanogenerators. Nat. Commun. 12, 4374. https://doi.org/10.1038/s41467-021-24417-w.
Saed, M.O., Ambulo, C.P., Kim, H., De, R., Raval, V., Searles, K., Siddiqui, D.A., Cue, J.M. O., Stefan, M.C., Shankar, M.R., Ware, T.H., 2019. Molecularly-engineered, 4D-printed liquid crystal elastomer actuators. Adv. Funct. Mater. 29, 1806412 https://doi.org/10.1002/adfm.201806412.
Sannino, A., Demitri, C., Madaghiele, M., 2009. Biodegradable cellulose-based hydrogels: design and applications. Materials 2, 353–373. https://doi.org/10.3390/ma2020353.
Sarkar, M., Upadhyay, A., Pandey, D., Sarkar, C., Saha, S., 2023. Cellulose-based biodegradable polymers: synthesis, properties, and their applications. In: Saha, S., Sarkar, C. (Eds.), Biodegradable Polymers and Their Emerging Applications, Mater. Horiz.: from Nature to Nanomaterials. Springer Nature, Singapore, pp. 89–114. https://doi.org/10.1007/978-981-99-3307-5_5.
Shah, T.V., Vasava, D.V., 2019. A glimpse of biodegradable polymers and their biomedical applications. E-Polymers 19, 385–410. https://doi.org/10.1515/epoly-2019-0041.
Shaikh, R., Raj Singh, T.R., Garland, M.J., Woolfson, A.D., Donnelly, R.F., 2011. Mucoadhesive drug delivery systems. J. Pharm. BioAllied Sci. 3, 89. https://doi.org/10.4103/0975-7406.76478.
Shen, Z., Chen, F., Zhu, X., Yong, K.-T., Gu, G., 2020. Stimuli-responsive functional materials for soft robotics. J. Mater. Chem. B 8, 8972–8991. https://doi.org/10.1039/D0TB01585G.
Shen, Q., Jiang, M., Wang, R., Song, K., Vong, M.H., Jung, W., Krisnadi, F., Kan, R., Zheng, F., Fu, B., Tao, P., Song, C., Weng, G., Peng, B., Wang, J., Shang, W., Dickey, M.D., Deng, T., 2023. Liquid metal-based soft, hermetic, and wireless-communicable seals for stretchable systems. Science 379, 488–493. https://doi.org/10.1126/science.ade7341.
Shi, Z., Zheng, F., Zhou, Z., Li, M., Fan, Z., Ye, H., Zhang, S., Xiao, T., Chen, L., Tao, T.H., Sun, Y.-L., Mao, Y., 2019. Silk-enabled conformal multifunctional bioelectronics for investigation of spatiotemporal epileptiform activities and multimodal neural encoding/decoding. Adv. Sci. 6, 1801617 https://doi.org/10.1002/advs.201801617.
Shigemitsu, H., Kubota, R., Nakamura, K., Matsuzaki, T., Minami, S., Aoyama, T., Urayama, K., Hamachi, I., 2020. Protein-responsive protein release of supramolecular/polymer hydrogel composite integrating enzyme activation systems. Nat. Commun. 11, 3859. https://doi.org/10.1038/s41467-020-17698-0.
Shin, J., Yan, Y., Bai, W., Xue, Y., Gamble, P., Tian, L., Kandela, I., Haney, C.R., Spees, W., Lee, Y., Choi, M., Ko, J., Ryu, H., Chang, J.-K., Pezhouh, M., Kang, S.-K., Won, S.M., Yu, K.J., Zhao, J., Lee, Y.K., MacEwan, M.R., Song, S.-K., Huang, Y., Ray, W.Z., Rogers, J.A., 2019. Bioresorbable pressure sensors protected with thermally grown silicon dioxide for the monitoring of chronic diseases and healing processes. Nat. Biomed. Eng. 3, 37–46. https://doi.org/10.1038/s41551-018-0300-4.
Shou, Y., Teo, X.Y., Li, X., Zhicheng, L., Liu, L., Sun, X., Jonhson, W., Ding, J., Lim, C.T., Tay, A., 2023. Dynamic magneto-softening of 3D hydrogel reverses malignant transformation of cancer cells and enhances drug efficacy. ACS Nano 17, 2851–2867. https://doi.org/10.1021/acsnano.2c11278.
Simon, D.M., Charkhkar, H., St John, C., Rajendran, S., Kang, T., Reit, R., Arreaga-Salas, D., McHail, D.G., Knaack, G.L., Sloan, A., Grasse, D., Dumas, T.C., Rennaker, R.L., Pancrazio, J.J., Voit, W.E., 2017. Design and demonstration of an intracortical probe technology with tunable modulus. J. Biomed. Mater. Res., Part A 105, 159–168. https://doi.org/10.1002/jbm.a.35896.
Someya, T., Bao, Z., Malliaras, G.G., 2016. The rise of plastic bioelectronics. Nature 540, 379–385. https://doi.org/10.1038/nature21004.
Song, K.-I., Seo, H., Seong, D., Kim, S., Yu, K.J., Kim, Y.-C., Kim, J., Kwon, S.J., Han, H.-S., Youn, I., Lee, H., Son, D., 2020. Adaptive self-healing electronic epineurium for chronic bidirectional neural interfaces. Nat. Commun. 11, 4195. https://doi.org/10.1038/s41467-020-18025-3.
Su, W., Darkwa, J., Kokogiannakis, G., 2015. Review of solid–liquid phase change materials and their encapsulation technologies. Renew. Sustain. Energy Rev. 48, 373–391. https://doi.org/10.1016/j.rser.2015.04.044.
Sun, J.-Y., Zhao, X., Illeperuma, W.R.K., Chaudhuri, O., Oh, K.H., Mooney, D.J., Vlassak, J.J., Suo, Z., 2012. Highly stretchable and tough hydrogels. Nature 489, 133–136. https://doi.org/10.1038/nature11409.
Sun, X., Guo, R., Yuan, B., Wang, H., Duan, M., Yang, Y., Zhu, X., Wang, X., Chen, S., Cheng, J., Fan, Y., Liu, J., 2022. Stiffness tunable implanted electrode enabled by magnetic liquid metal for wireless hyperthermia. Appl. Mater. Today 27, 101495. https://doi.org/10.1016/j.apmt.2022.101495.
Sunwoo, S.-H., Ha, K.-H., Lee, S., Lu, N., Kim, D.-H., 2021. Wearable and implantable soft bioelectronics: device designs and material strategies. Annu. Rev. Chem. Biomol. Eng. 12, 359–391. https://doi.org/10.1146/annurev-chembioeng-101420-024336.
Toma, M., Jonas, U., Mateescu, A., Knoll, W., Dostalek, J., 2013. Active control of SPR by thermoresponsive hydrogels for biosensor applications. J. Phys. Chem. C 117, 11705–11712. https://doi.org/10.1021/jp400255u.
Wang, S., Urban, M.W., 2020. Self-healing polymers. Nat. Rev. Mater. 5, 562–583. https://doi.org/10.1038/s41578-020-0202-4.
Wang, L., Yang, Y., Chen, Y., Majidi, C., Iida, F., Askounis, E., Pei, Q., 2018. Controllable and reversible tuning of material rigidity for robot applications. Mater. Today 21, 563–576. https://doi.org/10.1016/j.mattod.2017.10.010.
Wang, W., Wang, F., Zhang, C., Wang, Z., Tang, J., Zeng, X., Wan, X., 2020a. Robust, reprocessable, and reconfigurable cellulose-based multiple shape memory polymer enabled by dynamic metal–ligand bonds. ACS Appl. Mater. Interfaces 12, 25233–25242. https://doi.org/10.1021/acsami.9b13316.
Wang, Zijun, Wang, Zhijian, Zheng, Y., He, Q., Wang, Y., Cai, S., 2020b. Three-dimensional printing of functionally graded liquid crystal elastomer. Sci. Adv. 6, eabc0034 https://doi.org/10.1126/sciadv.abc0034.

Wang, H., Chen, S., Zhu, X., Yuan, B., Sun, X., Zhang, J., Yang, X., Wei, Y., Liu, J., 2022. Phase transition science and engineering of gallium-based liquid metal. Matter 5, 2054–2085. https://doi.org/10.1016/j.matt.2022.05.031.

Wang, Q., Pan, C., Zhang, Y., Peng, L., Chen, Z., Majidi, C., Jiang, L., 2023. Magnetoactive liquid-solid phase transitional matter. Matter 6, 855–872. https://doi.org/10.1016/j.matt.2022.12.003.

Ware, T., Simon, D., Arreaga-Salas, D.E., Reeder, J., Rennaker, R., Keefer, E.W., Voit, W., 2012a. Fabrication of responsive, softening neural interfaces. Adv. Funct. Mater. 22, 3470–3479. https://doi.org/10.1002/adfm.201200200.

Ware, T., Simon, D., Hearon, K., Liu, C., Shah, S., Reeder, J., Khodaparast, N., Kilgard, M. P., Maitland, D.J., Rennaker II, R.L., Voit, W.E., 2012b. Three-dimensional flexible electronics enabled by shape memory polymer substrates for responsive neural interfaces. Macromol. Mater. Eng. 297, 1193–1202. https://doi.org/10.1002/mame.201200241.

Ware, T., Simon, D., Liu, C., Musa, T., Vasudevan, S., Sloan, A., Keefer, E.W., Rennaker II, R.L., Voit, W., 2014. Thiol-ene/acrylate substrates for softening intracortical electrodes. J. Biomed. Mater. Res. Part B: Applied Biomaterials 102, 1–11. https://doi.org/10.1002/jbmb.32946.

Wen, X., Wang, B., Huang, S., Liu, T., Leo, Lee, M.-S., Chung, P.-S., Chow, Y.T., Huang, I.-W., Monbouquette, H.G., Maidment, N.T., Chiou, P.-Y., 2019. Flexible, multifunctional neural probe with liquid metal enabled, ultra-large tunable stiffness for deep-brain chemical sensing and agent delivery. Biosens. Bioelectron. 131, 37–45. https://doi.org/10.1016/j.bios.2019.01.060.

Wichterle, O., Lím, D., 1960. Hydrophilic gels for biological use. Nature 185, 117–118. https://doi.org/10.1038/185117a0.

Xu, K., Fu, Y., Chung, W., Zheng, X., Cui, Y., Hsu, I.C., Kao, W.J., 2012. Thiol–ene-based biological/synthetic hybrid biomatrix for 3-D living cell culture. Acta Biomater. 8, 2504–2516. https://doi.org/10.1016/j.actbio.2012.03.049.

Xu, S., Zhou, Z., Liu, Z., Sharma, P., 2023a. Concurrent stiffening and softening in hydrogels under dehydration. Sci. Adv. 9, eade3240 https://doi.org/10.1126/sciadv.ade3240.

Xu, Y., Su, Y., Xu, X., Arends, B., Zhao, G., Ackerman, D.N., Huang, H., Reid, StP., Santarpia, J.L., Kim, C., Chen, Z., Mahmoud, S., Ling, Y., Brown, A., Chen, Q., Huang, G., Xie, J., Yan, Z., 2023b. Porous liquid metal–elastomer composites with high leakage resistance and antimicrobial property for skin-interfaced bioelectronics. Sci. Adv. 9, eadf0575 https://doi.org/10.1126/sciadv.adf0575.

Xue, Y., Lei, J., Liu, Z., 2022. A thermodynamic constitutive model for shape memory polymers based on phase transition. Polymer 243, 124623. https://doi.org/10.1016/j.polymer.2022.124623.

Yang, S.Y., O'Cearbhaill, E.D., Sisk, G.C., Park, K.M., Cho, W.K., Villiger, M., Bouma, B. E., Pomahac, B., Karp, J.M., 2013. A bio-inspired swellable microneedle adhesive for mechanical interlocking with tissue. Nat. Commun. 4, 1702. https://doi.org/10.1038/ncomms2715.

Yang, Q., Liu, T.-L., Xue, Y., Wang, H., Xu, Y., Emon, B., Wu, M., Rountree, C., Wei, T., Kandela, I., Haney, C.R., Brikha, A., Stepien, I., Hornick, J., Sponenburg, R.A., Cheng, C., Ladehoff, L., Chen, Y., Hu, Z., Wu, C., Han, M., Torkelson, J.M., Kozorovitskiy, Y., Saif, M.T.A., Huang, Y., Chang, J.-K., Rogers, J.A., 2022. Ecoresorbable and bioresorbable microelectromechanical systems. Nat. Electron. 5, 526–538. https://doi.org/10.1038/s41928-022-00791-1.

Yoo, S., Lee, J., Joo, H., Sunwoo, S.-H., Kim, S., Kim, D.-H., 2021. Wireless power transfer and telemetry for implantable bioelectronics. Adv. Healthcare Mater. 10, 2100614 https://doi.org/10.1002/adhm.202100614.

Yoshikawa, H.Y., Rossetti, F.F., Kaufmann, S., Kaindl, T., Madsen, J., Engel, U., Lewis, A. L., Armes, S.P., Tanaka, M., 2011. Quantitative evaluation of mechanosensing of cells on dynamically tunable hydrogels. J. Am. Chem. Soc. 133, 1367–1374. https://doi.org/10.1021/ja1060615.

Yu, R., Cornette de Saint-Cyr, L., Soussan, L., Barboiu, M., Li, S., 2021. Anti-bacterial dynamic hydrogels prepared from O-carboxymethyl chitosan by dual imine bond crosslinking for biomedical applications. Int. J. Biol. Macromol. 167, 1146–1155. https://doi.org/10.1016/j.ijbiomac.2020.11.068.

Yu, A., Zhu, M., Chen, C., Li, Y., Cui, H., Liu, S., Zhao, Q., 2024. Implantable flexible sensors for health monitoring. Adv. Healthcare Mater. 13, 2302460 https://doi.org/10.1002/adhm.202302460.

Yuk, H., Wu, J., Zhao, X., 2022. Hydrogel interfaces for merging humans and machines. Nat. Rev. Mater. 7, 935–952. https://doi.org/10.1038/s41578-022-00483-4.

Zare, Mina, Bigham, A., Zare, Mohamad, Luo, H., Rezvani Ghomi, E., Ramakrishna, S., 2021. pHEMA: an overview for biomedical applications. Int. J. Mol. Sci. 22, 6376. https://doi.org/10.3390/ijms22126376.

Zhang, Y., Li, Y., Liu, W., 2015. Dipole–dipole and H-bonding interactions significantly enhance the multifaceted mechanical properties of thermoresponsive shape memory hydrogels. Adv. Funct. Mater. 25, 471–480. https://doi.org/10.1002/adfm.201401989.

Zhang, H., Guo, X., Wu, J., Fang, D., Zhang, Y., 2018a. Soft mechanical metamaterials with unusual swelling behavior and tunable stress-strain curves. Sci. Adv. 4, eaar8535 https://doi.org/10.1126/sciadv.aar8535.

Zhang, Q., Shi, C.-Y., Qu, D.-H., Long, Y.-T., Feringa, B.L., Tian, H., 2018b. Exploring a naturally tailored small molecule for stretchable, self-healing, and adhesive supramolecular polymers. Sci. Adv. 4, eaat8192 https://doi.org/10.1126/sciadv.aat8192.

Zhang, Y., Wang, Z., Yang, Y., Chen, Q., Qian, X., Wu, Y., Liang, H., Xu, Y., Wei, Y., Ji, Y., 2020. Seamless multimaterial 3D liquid-crystalline elastomer actuators for next-generation entirely soft robots. Sci. Adv. 6, eaay8606 https://doi.org/10.1126/sciadv.aay8606.

Zhang, P., Wang, N., Ren, D., Jing, Z., Sekhar, K.P.C., Hao, J., Cui, J., 2023a. Cascade reaction of thiol–disulfide exchange potentiates rapid fabrication of polymer hydrogels. ACS Macro Lett. 12, 1437–1442. https://doi.org/10.1021/acsmacrolett.3c00482.

Zhang, X., Gan, J., Fan, L., Luo, Z., Zhao, Y., 2023b. Bioinspired adaptable indwelling microneedles for treatment of diabetic ulcers. Adv. Mater. 35, 2210903 https://doi.org/10.1002/adma.202210903.

Zhang, Y., Lee, G., Li, S., Hu, Z., Zhao, K., Rogers, J.A., 2023c. Advances in bioresorbable materials and electronics. Chem. Rev. 123, 11722–11773. https://doi.org/10.1021/acs.chemrev.3c00408.

Zhao, Q., Qi, H.J., Xie, T., 2015. Recent progress in shape memory polymer: new behavior, enabling materials, and mechanistic understanding. Progr. Polym. Sci., Self-Healing Polym. 49–50, 79–120. https://doi.org/10.1016/j.progpolymsci.2015.04.001.

Zhao, R., Yao, Y., Luo, Y., 2016. Development of a variable stiffness over tube based on low-melting-point-alloy for endoscopic surgery. J. Med. Devices 10. https://doi.org/10.1115/1.4032813.

Zhao, Z., Liu, Y., Zhang, K., Zhuo, S., Fang, R., Zhang, J., Jiang, L., Liu, M., 2017a. Biphasic synergistic gel materials with switchable mechanics and self-healing capacity. Ange. Chem. Int 13464–13469. https://doi.org/10.1002/anie.201707239. Ed. 56.

Zhao, Z., Zhang, K., Liu, Y., Zhou, J., Liu, M., 2017b. Highly stretchable, shape memory organohydrogels using phase-transition microinclusions. Adv. Mater. 29, 1701695 https://doi.org/10.1002/adma.201701695.

Zhou, Y., Gu, C., Liang, J., Zhang, B., Yang, H., Zhou, Z., Li, M., Sun, L., Tao, T.H., Wei, X., 2022. A silk-based self-adaptive flexible opto-electro neural probe. Microsyst. Nanoeng. 8, 1–12. https://doi.org/10.1038/s41378-022-00461-4.

Zhou, T., Yuk, H., Hu, F., Wu, J., Tian, F., Roh, H., Shen, Z., Gu, G., Xu, J., Lu, B., Zhao, X., 2023. 3D printable high-performance conducting polymer hydrogel for all-hydrogel bioelectronic interfaces. Nat. Mater. 22, 895–902. https://doi.org/10.1038/s41563-023-01569-2.

Ziemba, A.M., Woodson, M.C.C., Funnell, J.L., Wich, D., Balouch, B., Rende, D., Amato, D.N., Bao, J., Oprea, I., Cao, D., Bajalo, N., Ereifej, E.S., Capadona, J.R., Palermo, E.F., Gilbert, R.J., 2023. Development of a slow-degrading polymerized curcumin coating for intracortical microelectrodes. ACS Appl. Bio Mater. 6, 806–818. https://doi.org/10.1021/acsabm.2c00969.

Zong, J., He, Q., Liu, Y., Qiu, M., Wu, J., Hu, B., 2022. Advances in the development of biodegradable coronary stents: a translational perspective. Mater. Today Bio 16, 100368. https://doi.org/10.1016/j.mtbio.2022.100368.